Università di Pisa

Facoltà di Scienze Matematiche Fisiche e Naturali

Corso di Laurea Specialistica in Scienze Fisiche

Anno Accademico 2007 - 2008

Tesi di Laurea Specialistica

Towards a Theory of Complexity Matching

Candidato

Mirko Luković

Relatore

Prof. Paolo Grigolini

Contents

Summary

Today there is still much debate regarding the definition of a complex system and complexity. We limit ourselves to two-state systems which jump randomly from one state to another and thus give rise to a dichotomous stochastic process. Our definition of a complex system is based on two properties: power-law statistics and renewal. The former implies that the waiting time distribution for both states is an inverse-power law with a finite exponent. The latter is a property whereby the time of permanence in one state is completely independent from the time of permanence in the other. If the system obeys power-law statistics with an exponent smaller than 2, then it is not ergodic. If, on the other hand, the exponent is greater than 2, but smaller than 3, then and equilibrium condition exists, but the system can reside for a very long period of time in an out-of-equilibrium condition. Recently, it has been shown that the linear response of a complex system to a coherent perturbation vanishes in the long-time limit. This result, together with the hypothesis that complex systems can be excited only by other complex systems, is the key motivation for the work presented in this thesis. It is part of an ongoing search for a theory of complexity matching, a theory showing that complex systems respond only if they are excited by other complex systems and that otherwise the response is attenuated.

In the first part of the thesis we explore the possibility of coupling two Poisson processes. Our approach is based on the experience obtained in the field of stochastic resonance. We try to perturb a system that obeys ordinary Poisson statistics using Poissonian signals with different rates. To this end, we adopt a simple model that reproduces aperiodic stochastic resonance and we show that such a phenomenon is

not present in the more general case in which the rate is not necessarily induced by some kind of noise. Furthermore, we adopt the concept of events and use it to study the interaction of Poisson systems. We discover that, when the system produces events at a lower rate with respect to the perturbation, the events of the perturbation become attractors of the system events and vice versa. We use the term rate matching to identify the condition when the two rates of event production are the same.

The second part of the thesis deals with signals produced by complex systems. In order to present the full theory of complexity matching, a new fluctuation-dissipation theorem must be introduced, but this goes beyond the scope of the work presented here. However, the understanding of the non-ergodic nature of complex systems is fundamental to the application of the new fluctuation dissipation theorem. Therefore, here we study the power spectrum of complex signals and show that $1/f$-noise is produced by systems that lie on the border that separates ergodic systems from non-ergodic ones. We do this by generalising the Wiener-Khinchin theorem and extending it to non-stationary non-ergodic processes. We distinguish between two different types of truncation effects: the physical truncation, where we use a truncated waiting time distribution, and an observation-induced effect, which is a consequence of finite acquisition times. It is the finite observation time that allows us to apply the generalised Wiener-Khinchin theorem in the non-ergodic case. Our final results show that the power spectrum is related to the frequency via an inverse power law and that, in the non-ergodic condition, the power spectrum also depends on the observation time.

CHAPTER 1

Introduction

We investigate systems that jump randomly between two well-defined states. The rate at which the jumps occur may depend on the absolute time. We assume that all the jumps are completely independent of one another so that each jump resets to zero the systems memory. We call this property *renewal*. Such systems produce a time series, $\xi(t)$, of some physical property that fluctuates between two values. For simplicity we shall assume that the two states are symmetric and that the sojourn times in each state are governed by a waiting time distribution $\psi(\tau)$. The form of such a distribution determines the nature of the system and the corresponding time series. There are two forms in particular that interest us:

$$\psi(\tau) = g \exp(-g\tau) \tag{1.1}$$

and

$$\psi(\tau) = (\mu - 1)\frac{T^{\mu-1}}{(T+\tau)^{\mu}}, \tag{1.2}$$

where g, μ and T are constant parameters that characterise the distributions. The first distribution is responsible for Poissonian processes and the parameter g determines the rate at which events occur [8]. The second distribution generates power-law statistics. Any system with renewal and a waiting time distribution equal to

the one in Eq. (1.2) will be considered *complex*. Our goal is to study the interaction of these complex systems. We are searching for a matching condition under which there is a maximal exchange of information between these systems. We call such a condition *complexity matching*. Nevertheless, research is still in progress and therefore only some aspects shall be presented in this thesis. Before considering complex systems, we studied the effects of coupling two Poisson systems. These systems are stationary and therefore much easier to deal with. The results are shown in the first part of the thesis. They have also been published recently in the journal "Physics Letters A" [9].

Chapter 2 is dedicated to the study of Poisson systems and their interaction. We start by presenting the phenomenon of stochastic resonance whereby a two-state system is perturbed by a sinusoidal signal. The important work done by McNamara and Wiesenfeld [11] makes it possible to understand the essence of the phenomenon, by essentially replacing the double-well system with a dichotomous Poisson process $\xi(t)$. We extend this idea by substituting the deterministic signal with a stochastic one, Poissonian, to be precise. The stochastic nature of the perturbation, $\xi_P(t)$, forces us to use the Gibbs ensemble approach whereby many realisations of the same process are used. Here we present our first important result, the *rate matching* condition. We discover that, when the system produces events at a lower rate with respect to the perturbation, the events of the perturbation become attractors of the system events and vice versa.

In chapter 3 we analyse the power spectra of stochastic processes that obey power-law statistics. The main theme of this, second, part of the thesis is the fact that systems characterised by $\mu = 2$ reside on the border that separates ergodic from non-ergodic systems. We show that the power spectrum produced by such systems has the form $1/f$ and that more generally, for $1 < \mu < 3$, the power spectrum is given by

$$S(f) \propto \frac{1}{f^{3-\mu}}. \tag{1.3}$$

We generalise the Wiener-Khinchin theorem and use it to calculate the power spectra of finite non-ergodic processes. We consider this result important because there is a lot of empirical evidence that shows that there is communication between $1/f$ noise systems. For example, Mutch [2] proved that a ventilator tuned to the $1/f$ nature of the breathing process is much more efficient than ordinary ventilators. There is

experimental evidence that a $1/f$ noise system is more sensitive to $1/f$ noise than to white noise: The brain is proven to be sensitive to $1/f$ noise much more than to white noise [3]. The work of Buiatti et al. [5] proves that the brain, as well as music and painting, is a source of $1/f$ noise, in accordance with [6]. The brain generates $1/f$ noise and so do the psycho-physiological processes under the brains control [7]. Finally, we show that in the non-ergodic case, the power spectrum depends also on the duration, L, of the process. For a fixed frequency, f_0, we have that

$$S(f_0, L) \propto \frac{1}{L^{2-\mu}}. \tag{1.4}$$

CHAPTER 2

Rate Matching

2.1 Stochastic Resonance

The well-known phenomenon of stochastic resonance [12] rests on the apparently non-intuitive notion that an increase in noise intensity improves the transition of a signal. We are not going to discuss stochastic resonance in detail; we just want to present the essentials that will be useful for studying the interaction of two Poissonian systems.

Originally, the phenomenon was studied using systems composed of a particle in a bistable double-well potential. We start by analysing such a system when it is subjected to thermal noise and perturbed by a periodic signal. The equation of motion is given by the Langevin equation

$$\begin{aligned} \dot{x} &= v \\ \dot{v} &= -\gamma v - \frac{\partial V}{\partial x} + \xi(t) + \varepsilon \cos(\omega_0 t) \end{aligned} \tag{2.1}$$

Here $\xi(t)$ denotes a Gaussian white noise with zero average and autocorrelation function $\langle \xi(t)\xi(t') \rangle = 2\gamma k_B T \delta(t - t')$. For simplicity, we consider a symmetric potential, $V(x)$ (see Fig. (2.1)), and a particle with mass, $m = 1$. In the absence of periodic

forcing, the noise causes the particle to jump randomly over the potential barrier from one well into the other. We assume that the signal amplitude, ε, is small enough so that in the absence of any noise, it is insufficient to force the particle over the potential barrier.

For very large values of γ (overdamped approximation), $\dot{v} = 0$ and

$$\dot{x} = -\frac{1}{\gamma}\frac{\partial V}{\partial x} + \frac{\xi(t)}{\gamma} + \varepsilon\frac{\cos(\omega_0 t)}{\gamma}. \tag{2.2}$$

The position of the particle $x(t)$ is considered to be the output of the system. In the absence of modulation ($\varepsilon = 0$), $x(t)$ fluctuates around its local stable states ($x = \pm a$) with a statistical variance proportional to the noise intensity $\gamma k_B T$. In the overdamped approximation, the inter-well transition rate is given by the Kramers rate [10, 22]

$$q = \frac{\omega_a \omega_m}{2\pi\gamma} \exp\left(-\frac{V_0}{k_B T}\right) \tag{2.3}$$

where $\omega_a^2 = V''(a)$ is the squared angular frequency of the potential in the potential minima at $\pm a$, and $\omega_m^2 = |V''(0)|$ the squared angular frequency at the top of the barrier, located in $x = 0$. We can now say that in the overdamped approximation, $\gamma \gg \omega_m$. Originally, Kramers considered a Brownian particle caught in a potential well. He calculated the escape rate of the particle over the potential barrier, and used his result in the theory of the velocity of chemical reactions [10]. Because the expression for the Kramers transition rate depends only on the potential barrier height, V_0, and the curvature of the potential at the maximum and minima, it is not necessary that we know the exact form of the potential, $V(x)$. The height of the barrier has to be much greater than the mean (thermal) energy of the particle otherwise it would diffuse more or less freely from one well to the other. Also, if it were of comparable height, the time scales for equilibrium and escape would not be clearly separated. The perturbative force $\varepsilon\cos(\omega_0 t)$ modifies the double-well potential producing

$$V^{eff}(x,t) = V(x) + \varepsilon x\cos(\omega_0 t). \tag{2.4}$$

In that case, the barrier height changes too,

$$\Delta V^{eff}(t) = V_0 + \varepsilon a \cos(\omega_0 t) \tag{2.5}$$

and the perturbed Kramers rate is given by

$$q_{\pm}(t) = \frac{\omega_a \omega_m}{2\pi\gamma} \exp\left\{-\frac{V_0 \pm \varepsilon a \cos(\omega_0 t)}{k_B T}\right\} = q \exp\left(\mp \frac{\varepsilon a}{k_B T} \cos(\omega_0 t)\right). \tag{2.6}$$

The Kramers rate formula is derived under the assumption that the probability

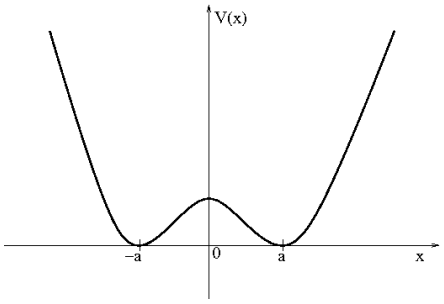

Figure 2.1: This is an example of a typical double well potential. Depending on the amount of kinetic energy possessed by the particle, it may be able to jump over the barrier, from one well to the other.

density within a well is roughly at equilibrium, a Gaussian distribution centred about the minimum. Thus, in order to use Eq.(2.6), the signal frequency must be much slower than the characteristic rate for probability to equilibrate within a well. This rate is the curvature of the well minimum and therefore the adiabatic limit is valid only for $\omega_0 \ll \omega_a$. On assuming that the modulation amplitude is small, i.e. $\varepsilon a \ll k_B T$, we can use the following expansion in the small parameter $\varepsilon a/(k_B T)$,

$$q_{\pm} = q\left(1 \mp \frac{\varepsilon a}{k_B T} \cos(\omega_0 t) + \ldots\right) \simeq q\left(1 \mp \eta \cos(\omega_0 t)\right). \tag{2.7}$$

Before we procede with the calculation of the expectation value of $x(t)$, we introduce the concept of events. It is not an essential part of stochastic resonance but will be very useful in the next chapter.

Whenever the particle reaches the top of the potential barrier we shall say that an *event* has occurred. Nevertheless, this does not mean that the system has changed its state. When the particle reaches the top of the barrier it can either fall back to

the bottom of the well from which it started or it can continue and jump into the other well. We shall assume that these to scenarios have the same probability of occurring. Since the particle has the same probability of falling back or continuing into the other well, we can interpret the outcome as the result of a coin toss. If the particle manages to jump into the other well after it has reached to top of the barrier, we shall say that a *collision* has occurred. In other words, a collision causes the system to change its state. Note that many events can occur before a single collision. The particle may reach the top several times before it actually manages to advance into the other well, and thus convert the final event into a collision. The probability that a collision occurs after n events is given by $(1/2)^{n+1}$. In this case, the $(n+1)^{th}$ event is converted into a collision. It is the same as saying that the particle moves randomly in a single well, reaching the top n times before actually making the jump into the other well at the $(n+1)^{th}$ attempt. If we use the new rate,

$$g = 2q, \tag{2.8}$$

together with the coin-tossing procedure, then the correlation function of the corresponding process will be equal to the correlation function related to the Kramers rate, q. The proof of this statement shall postponed until subsection 3.2.2.

In the presence of a moderate amount of random forcing and heavy damping, the particle will spend most of its time at the bottom of the wells, near $x = \pm a$, making occasional transitions over the barrier. We have already mentioned that the exact shape of the potential is not important for the study of the dynamics of the system. Following McNamara and Wiesenfeld [11], we substitute the double-well with an arbitrary two-state system and maintain the Kramers transition rate shown in Eq. (2.3). We assume that the particle can occupy only two discrete states. For example, we shall assume that the particle occasionally jumps from the position $x = a$ to $x = -a$ and vice versa. In order to calculate the expectation value of $x(t)$, we can procede by using the following master equation (the system has two states and hence the master equation proves to be an effective tool). P_1 and P_2 are the

probabilities of finding the particle in the position $x = a$ and $x = -a$ respectively.

$$\begin{aligned}\frac{d}{dt}P_1 &= -\frac{g_+(t)}{2}P_1 + \frac{g_-(t)}{2}P_2 \\ \frac{d}{dt}P_2 &= -\frac{g_-(t)}{2}P_2 + \frac{g_+(t)}{2}P_1.\end{aligned} \tag{2.9}$$

The factor $1/2$ present in the master equation reflects the fact that g is the rate at which the particle reaches the top of the potential barrier and not the rate at which it overcomes it. When it is at the top of the barrier, the particle may either overcome it or it may return to its original position. Both cases are equally likely and that is why we need the factor $1/2$. In order to resolve the master equation we introduce the variable

$$\Pi(t) = P_1(t) - P_2(t) \tag{2.10}$$

and substitute it into (2.9). After some simplifications we obtain

$$\dot{\Pi}(t) = -\frac{g_+ + g_-}{2}\Pi(t) + \frac{g_- - g_+}{2}. \tag{2.11}$$

Substituting (2.7) into (2.11)

$$\dot{\Pi}(t) = -g\Pi(t) - g\eta\cos(\omega_0 t). \tag{2.12}$$

We can find the solution of the master equation by using $\exp(gt)$ as the integrating factor in the first order differential equation. We get

$$\Pi(t) = -g\eta\int_0^t e^{-g(t-t')}\cos(\omega_0 t')dt' + \Pi(0)e^{-gt}. \tag{2.13}$$

From the definition for the expectation value over a Gibbs ensemble, we have that

$$\langle x(t)\rangle = a\Pi(t), \tag{2.14}$$

and therefore

$$\Pi(0) = \frac{\langle x(0)\rangle}{a}. \tag{2.15}$$

We shall assume that the system starts from equilibrium, in which case $\Pi(0) = 0$. This means that before we apply the perturbation, the expectation value of the output is zero for every t. The expectation value of $x(t)$ is obtained by calculating the integral in (2.13).

$$\begin{aligned}\int_0^t e^{-g(t-t')}\cos(\omega_0 t')dt' &= e^{-gt}\int_0^t e^{gt'}\frac{e^{i\omega_0 t'}+e^{-i\omega_0 t'}}{2}dt' \\ &= \frac{e^{-gt}}{2}\left\{\frac{e^{(g+i\omega_0)t}-1}{g+i\omega_0}+\frac{e^{(g-i\omega_0)t}-1}{g-i\omega_0}\right\}. \end{aligned} \tag{2.16}$$

Since the Poisson system needs time to adapt, we study the limit where $t \gg 1/g$ and consequently $\exp(-gt) \to 0$, the system . In that case,

$$\begin{aligned}\Pi(t) &= -g\frac{\eta}{2}\left[\frac{e^{i\omega_0 t}}{g+i\omega_0}+\frac{e^{-i\omega_0 t}}{g-i\omega_0}\right] \\ &= -\frac{g\eta}{2(g^2+\omega_0^2)}\left[(g-i\omega_0)(\cos(\omega_0 t)+i\sin(\omega_0 t))+(g+i\omega_0)(\cos(\omega_0 t)-i\sin(\omega_0 t))\right] \\ &= -g\eta\frac{1}{g^2+\omega_0^2}(g\cos(\omega_0 t)+\omega_0\sin(\omega_0 t)) \\ &= -\frac{g\eta}{g^2+\omega_0^2}\left[\sqrt{g^2+\omega_0^2}\sin\phi\cos(\omega_0 t)+\sqrt{g^2+\omega_0^2}\cos\phi\sin(\omega_0 t)\right] \\ &= -g\eta\frac{1}{\sqrt{g^2+\omega_0^2}}\cos(\omega_0 t+\phi). \end{aligned} \tag{2.17}$$

In conclusion, when the system adapts itself to the perturbation,

$$\langle x(t)\rangle = -aC\cos(\omega_0 t-\phi), \tag{2.18}$$

where

$$C = \frac{g\eta}{\sqrt{g^2+\omega_0^2}} \quad \text{and} \quad \tan\phi = \frac{g}{\omega_0}. \tag{2.19}$$

Note that when we switch off the perturbation ($\varepsilon = 0$) the expectation value is zero, just as we mentioned earlier. Since (see Eq.(2.3))

$$g = 2q = 2\frac{\omega_a\omega_m}{2\pi\gamma}\exp\left(-\frac{V_0}{k_BT}\right) \quad \text{and} \quad \eta = \frac{\varepsilon a}{k_BT}, \tag{2.20}$$

we have that

$$C(T) = 2A \exp\left(-\frac{V_0}{k_B T}\right) \cdot \frac{\varepsilon a}{k_B T} \cdot \left[4A^2 \exp\left(-2\frac{V_0}{k_B T}\right) + \omega_0^2\right]^{-\frac{1}{2}}, \tag{2.21}$$

where $A = \omega_a \omega_m/(2\pi\gamma)$. The graph of Eq. (2.21) is displayed in Fig. (2.2). Notice that the function has a maximum value. This maximum response of the system to the external perturbation is know as *stochastic resonance*. Sometimes it is useful to

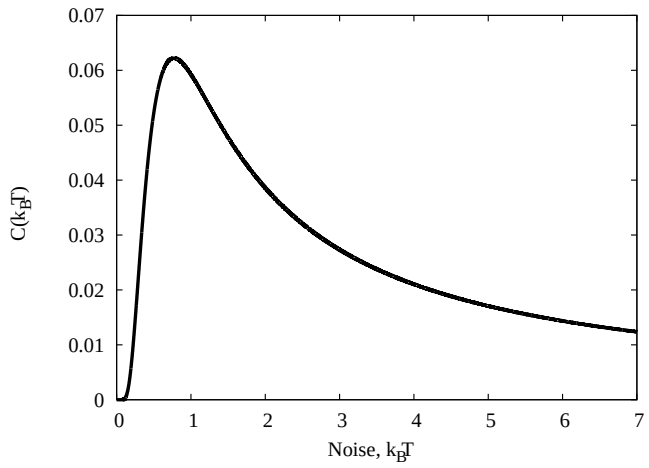

Figure 2.2: This graph is a plot of Eq. (2.21) with $\varepsilon = 0.1$ and with V_0, a, A, ω_0 all equal to unity. It shows that for a particular temperature, and consequently, for a certain amount of noise, the intensity of the output signal is maximum.

define stochastic resonance in terms of the signal-to-noise ration (SNR). Following Gammaitoni et al. [12], we present the following definition:

$$SNR = \frac{2}{S_N(\omega_0)} \left[\lim_{\Delta\omega \to 0} \int_{\omega_0 - \Delta\omega}^{\omega_0 + \Delta\omega} S(\omega) d\omega\right], \tag{2.22}$$

where $S(\omega)$ is the power spectral density (power spectrum from now on) of $x(t)$. The periodic component of $x(t)$ contributes to $S(\omega)$ with a series of delta spikes centred at $\omega = (2n+1)\omega_0$ with $n = 0, \pm 1, \pm 2, \ldots$. Therefore, $S_N(\omega)$ is the total power spectrum minus the delta spikes; it is the background power spectrum. For small forcing amplitudes, $a\varepsilon \ll V_0$, the $S_N(\omega)$ is not very different from the power

spectrum of the unperturbed system. In that case

$$S_N(\omega) \approx 2\int_0^\infty \langle x_{_N}(t)x_{_N}(t+\tau)\rangle \cos(\omega\tau)d\tau = 2a^2\int_0^\infty e^{-g\tau}\cos(\omega\tau)d\tau$$
$$= 2a^2\frac{g}{g^2+\omega^2}, \tag{2.23}$$

where $x_{_N}(t)$ is the output produced in the absence of the periodic signal.

$$S(\omega) = \frac{\pi}{2}a^2C^2[\delta(\omega-\omega_0)+\delta(\omega+\omega_0)] + S_N(\omega). \tag{2.24}$$

The signal-to-noise ratio is given by (in first approximation),

$$SNR \approx \frac{\pi}{2}\left(\frac{\varepsilon a}{k_BT}\right)^2 g = \pi\left(\frac{\varepsilon a}{k_BT}\right)^2 A\exp\left(-\frac{V_0}{k_BT}\right). \tag{2.25}$$

Fig. (2.3) shows that the signal-to-noise ratio has a maximum similar to the one seen in the case of the amplitude. However, note that the noise intensity at which SNR assumes its maximum does not coincide with the value k_BT that maximises the response amplitude C.

2.2 Rate Matching

We have seen that stochastic resonance is the result of statistical synchronisation, which takes place when the average waiting time, $1/g$, between two interwell transitions is comparable with half the period of the periodic forcing. This yields the time-scale matching condition for stochastic resonance,

$$\frac{1}{g} = \frac{1}{2}\frac{2\pi}{\omega_0} \Rightarrow g = \frac{\omega_0}{\pi}. \tag{2.26}$$

Stochastic resonance involves a Poisson system that is perturbed by a periodic signal. However, Eq. (2.6), and all the subsequent approximations, can be used even when the forcing signal (perturbation) is not a deterministic function of time. We are now going to adopt the approach introduced by McNamara and Wiesenfeld [11]. We consider a two-state system that jumps randomly from one state to the other, without paying attention to the physical details, just the essential properties: Pois-

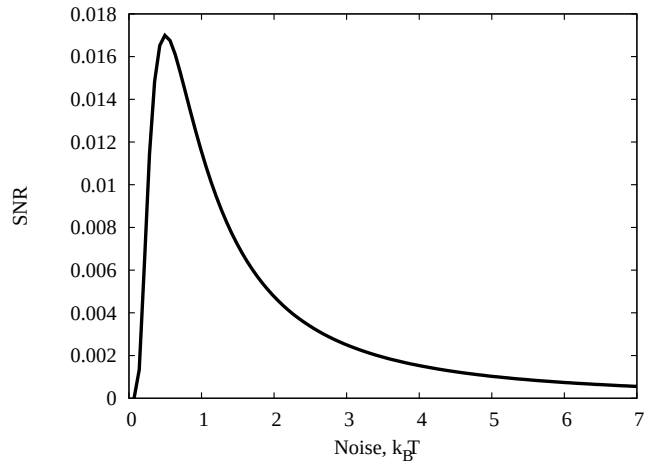

Figure 2.3: This figure shows the plot of Eq. (2.25) with $\varepsilon = 0.1$ and V_0, a, A all equal to unity. There is also a maximum when we consider the signal-to-noise ratio. However, the value of T for which the maximum occurs does not coincide with the temperature that produces the maximum in Fig. (2.2).

son waiting time distribution and the hopping rate g_S. Generalising even further, we shall assume that g_S is an arbitrary rate, not the noise-induced Kramers rate of Eq. (2.3). As for the perturbation, we consider a dichotomous signal with random fluctuations that obey Poisson statistics with rate g_P. So, we have a situation where a stochastic signal $\xi_P(t)$ with rate g_P is used to perturb a two-state system, which, in the absence of the perturbation, jumps randomly form one state to the other at a rate g_S. For simplicity, we assume that the two states are $|+\rangle = +1$ and $|-\rangle = -1$. Since we are not going to involve the Kramers rate, we have to generalise Eq. (2.6), in which the perturbation intensity η depends on the thermal noise. From now on, we are going to use ε as the perturbation intensity with the assumption that it is arbitrary and dimensionless. Hence, the generalised interaction will mediated through

$$g_{\pm}(t) = g_S(1 \pm \varepsilon\xi_P(t)). \tag{2.27}$$

When the system is in state $|+\rangle$, the transition rate is $g_+(t) = g_S(1 + \varepsilon\xi_P(t))$ and similarly for the state $|-\rangle$. The output, $\xi_S(t)$, will also be a dichotomous function of time. The perturbation, $\xi_P(t)$, modifies only the rate g_S of the system and not

its two states so that the output, $\xi_S(t)$ will still fluctuate between the two values $+1$ and -1. The output can be calculated using the master equation in Eq. (2.9) together with the rate in (2.27). By following the steps seen in the previous section, we find that

$$\Pi(t) = g_S\varepsilon \int_0^t e^{-g_S(t-t')}\xi_P(t')dt'. \tag{2.28}$$

It is obvious that if we use $\xi_P(t)$, the mean response, $\Pi(t) = \langle \xi_S(t) \rangle$ is a stochastic function of time. In order to make analytical predictions we have to move from the single realisation of $\xi_P(t)$ to the realisation of infinitely many $\xi_P(t)$ that share the same initial value. Thus, we assume that every realisation of the perturbation satisfies the condition $\xi_P(0) = 1$. Otherwise, we would have $\langle \xi_P(t) \rangle = 0$. Using Eq. (2.28), we obtain the two-fold expectation value

$$\langle \Pi(t) \rangle_P = \langle \langle \xi_S(t) \rangle_S \rangle_P = g_S\varepsilon \int_0^t e^{-g_S(t-t')} \langle \xi_P(t') \rangle_P dt'. \tag{2.29}$$

The condition $\xi_P(0) = 1$ shared by all realisations of $\xi_P(t)$, yields

$$\langle \xi(t') \rangle_P = \exp(-g_P t). \tag{2.30}$$

By substituting (3.1) into (2.28) we have

$$\langle \langle \xi_S(t) \rangle_S \rangle_P = g_S\varepsilon \int_0^t e^{-g_S(t-t')} e^{-g_P t'} dt' \tag{2.31}$$

and after some straightforward algebra

$$\langle \langle \xi_S(t) \rangle_S \rangle_P = \frac{g_S\varepsilon}{g_S - g_P} \left[\exp(-g_P t) - \exp(-g_S t) \right]. \tag{2.32}$$

A particular case of the function $\langle \Pi(t) \rangle_P$ is shown in Fig. (2.4). The fact that $\langle \Pi(t) \rangle_P$ decays can mean two things: Either the single output means $\langle \xi_S(t) \rangle_S$ decay themselves or they fluctuate in such a way that when we sum them up, the resultant decays. We shall now show that the latter case is true. We take a closer look at Eq. (2.32) and consider the two limits, $g_S \ll g_P$ and $g_S \gg g_P$. In the first case we have

$$\langle \Pi(t) \rangle_P = \varepsilon \frac{g_S}{g_P} \exp(-g_S t), \tag{2.33}$$

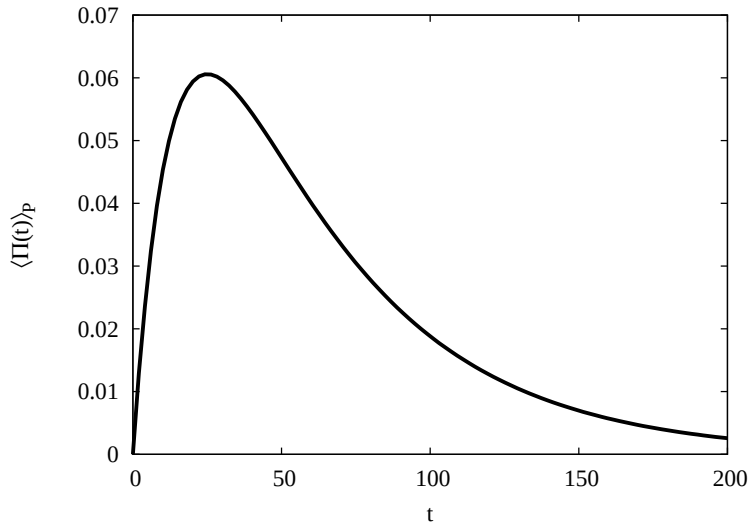

Figure 2.4: This figure shows a plot of Eq. (2.32) with $g_S = 0.07$, $g_P = 0.02$ and $\varepsilon = 0.1$.

and in the second case

$$\langle \Pi(t) \rangle_P = \varepsilon \exp(-g_P t). \tag{2.34}$$

Before proceeding, we have to remind ourselves that in the absence of perturbation $\langle \Pi(t) \rangle_P = 0$. Therefore, the fact that $\langle \Pi(t) \rangle_P$ is different from zero implies that the perturbation has some effect on the system, regardless of the limit considered. By observing Eqs. (2.33) and (2.34) we can conclude that the perturbation is more effective when $g_S \gg g_P$. It is enough to look at the coefficients; the factor $\varepsilon g_S / g_P$ in Eq. (2.33) is much smaller than the coefficient ε in Eq. (2.34). Moreover, when $g_S \gg g_P$, $\langle \Pi(t) \rangle_P$ decays exponentially with the factor g_P, leading us to believe that in this case the system is able to reproduce the signal fairly well. Similarly, it is plausible that for $g_S \ll g_P$, the system is not able to reproduce the signal since the decay factor is g_S, therefore the output remains almost unchanged. We must not forget that an ensemble of Poisson processes with rate g decays exponentially with a factor g when we use the coin-tossing method. These deductions can be consolidated by considering the crosscorrelation between the perturbation and the system.

Following the authors of Ref. [45], we use the crosscorrelation function

$$C(t) \equiv \langle \xi_P(t)\xi_S(t)\rangle_{SP} \tag{2.35}$$

In order to get an analytical expression, we procede as before. We consider all the cases where the experiment was done with the same $\xi_P(t)$ and we make the average on all the resulting $\xi_S(t)$. Then we average over all the perturbation realisations. Thus, we write

$$C(t) = \langle \xi_P(t)\xi_S(t)\rangle_{SP} = \langle \langle \xi_S(t)\rangle_S \xi_P(t)\rangle_P. \tag{2.36}$$

We can now use Eq. (2.28) and by substituting it into the crosscorrelation function we get

$$C(t) = \varepsilon g_S \int_0^t \exp(-g_S(t-t'))\langle \xi_P(t')\xi_P(t)\rangle_P \, dt'. \tag{2.37}$$

By noting that

$$\langle \xi_P(t')\xi_P(t)\rangle_P = \exp(-g_P(t-t')), \tag{2.38}$$

we obtain

$$C(t) = \varepsilon g_S e^{-(g_S+g_P)t} \int_0^t e^{(g_S+g_P)t'} dt' = \frac{\varepsilon g_S}{g_S+g_P}\left[1 - e^{-(g_S+g_P)t}\right]. \tag{2.39}$$

We consider the asymptotic limit of the crosscorrelation function so that

$$\chi \equiv \lim_{t\to\infty} C(t) = \frac{\varepsilon g_S}{g_S+g_P}. \tag{2.40}$$

From Eq. (2.40) we can conclude that the maximum correlation ($\chi = \varepsilon$) occurs when $g_S \gg g_P$. The correlation parameter, χ, increases monotonically from 0 to ε and at $g_S = g_P$ no deviation from this monotonic behaviour appears. With the help of Eq. (2.40) we can conclude that the system reproduces the perturbation reasonably well in the case where $g_S \gg g_P$ and $t \to \infty$. In other words, $\langle \xi_S(t)\rangle_S \approx \varepsilon \xi_P(t)$. On the other hand, when $g_S \ll g_P$, the correlation is very poor or even absent. This tells us that the system is not able to reproduce the perturbation ξ_P. Nevertheless, the system does respond (very weakly, but it does respond) to a perturbation when

g_S is very small. The response is due to the short sojourn times produced by the system. Such times are very rare because the rate is very low, however, they are present. The fact that they are rare explains the weak response.

By deriving $\langle \Pi(t) \rangle_P$ and equating the result to zero we get

$$-g_P \exp(-g_P t) + g_S \exp(-g_S t) = 0. \tag{2.41}$$

Therefore, the maximum occurs at

$$t_M = \frac{\ln(g_P) - \ln(g_S)}{g_P - g_S}. \tag{2.42}$$

Substituting (2.42) into (2.32) yields the maximum:

$$\begin{aligned} \langle \Pi(t_M) \rangle_P &= \frac{g_S \varepsilon}{g_S - g_P} \left[\exp\left(-\frac{\ln(g_P/g_S)}{g_P - g_S} g_P \right) - \exp\left(-\frac{\ln(g_P/g_S)}{g_P - g_S} g_S \right) \right] \\ &= \frac{g_S \varepsilon}{g_S - g_P} \left[\left(\frac{g_P}{g_S} \right)^{-\frac{g_P}{g_P - g_S}} - \left(\frac{g_P}{g_S} \right)^{-\frac{g_S}{g_P - g_S}} \right] \\ &\equiv \frac{g_S \varepsilon}{g_S - g_P} \left[A^{-g_P} - A^{-g_S} \right], \end{aligned} \tag{2.43}$$

where

$$A = \left(\frac{g_P}{g_S} \right)^{\frac{1}{g_P - g_S}}. \tag{2.44}$$

If we fix the perturbation rate g_P and vary the system rate, $\langle \Pi(t_M) \rangle_P$ remains a monotonous function of g_S (see Fig. (2.5)). In conclusion, neither the cross-correlation $C(t)$ nor the maximum value of the output $\langle \Pi(t_M) \rangle_P$ produces a resonance effect. All calculations show that the amplitude and quality of the output increase monotonically as we increase the system rate g_S. In section 2.1 we considered the interaction between a Poisson system and a deterministic signal ($\cos(\omega_0 t)$). We saw that for a particular rate of the system, the output intensity had a maximum. However, it should be noted that the maximum is obtained as a consequence of the fact that the rate g is a non-linear function of $k_B T$. In fact, if we substitute the noise-induced Kramers rate with an arbitrary one and use a dimensionless

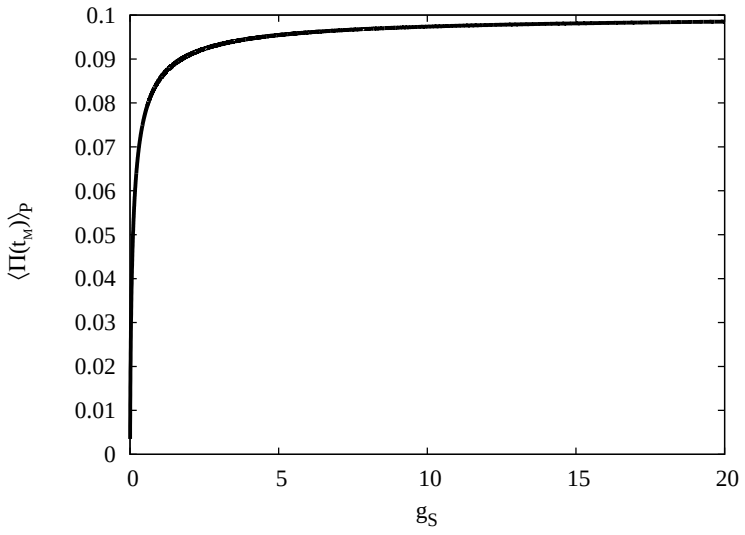

Figure 2.5: This figure shows a plot of Eq. (2.43) with $g_P = 0.05$ and $\varepsilon = 0.1$. It shows that $\langle \Pi(t_M) \rangle_P$ tends to ε as g_S increases.

perturbation intensity ε, we are left with the monotonous function in Eq. (2.19)

$$C(g) = \frac{g\varepsilon}{\sqrt{g^2 + \omega_0^2}}. \tag{2.45}$$

Stochastic resonance is present only if the rate is controlled in a specific way by some other physical quantity, such as the temperature.

2.2.1 Single Realisation

Let us now move from the Gibbs ensemble perspective to the observation of a single realisation of the perturbation-response process. We start by creating two different realisations of a set of laminar regions (representing the time distance between two consecutive events) that obey the *Poisson distribution*. Therefore each of the two realisations is characterised by a single, constant parameter, namely, the rate of events g. The realisation may possess different rates. One realisation is considered to be the perturbation, P, with a rate g_P and the other is considered to be the system, S, with a rate g_S. It has to be pointed out that the definition of an event used here is the same as the one given in section 2.1. In other words, an event

corresponds to the system reaching the barrier top. The experiment is realised as follows: We perturb S using P and we repeat the process by changing either g_S or g_P while the other rate is kept constant. We want to see whether there is some kind of an effect when we set the matching condition $g_P = g_S$. In order to establish which is the effect produced by *rate matching*, if any exists, we have to define a *marker*, R, which will reveal it. The simplest marker is realised using what we call the *time difference method*. We adopt the idea of the authors of Ref. [13], but without the entropic method. Instead, we use a simplified version adapted for our needs. The unperturbed system, S, is confronted with the perturbation and the time differences, t_n, are measured as shown in Fig. 2.6. We decide which of the two realisations will be the reference one and apply the following rule: for each event of the reference realisation we measure the time that it takes for the next event of the other realisation to occur. Let us say that we are considering the n^{th} event, E_n^{ref}, of the reference realisation; then we have to start measuring the time from E_n^{ref} and wait until an event of the other realisation occurs; we consider only the first neighbour. If no such event occurs before E_{n+1}^{ref} then the event E_n^{ref} is disregarded. The time interval measured in this way is the time difference that we are talking about and we shall denote it by the symbol t_n. All the time differences measured in this way are summed up so that we have

$$L_0 = \sum_{n=0}^{N} t_n, \tag{2.46}$$

where, N is the final event of the reference realisation and t_0 is always zero because both realisations are prepared in such a way that at time $t = 0$ they both have an event. The next thing to do is to repeat the above procedure. This time we apply the same procedure by switching on the interaction between S and P, namely by assigning a non-vanishing value to ε in Eq. (2.27). In this case, we denote the time differences t_n^P, $n = 0, 1, \ldots, N$ and we have

$$L_P = \sum_{n=0}^{N} t_n^P. \tag{2.47}$$

Finally, we define the marker

$$R = \frac{L_P}{L_0} = \frac{\sum_{n=0}^{N} t_n^P}{\sum_{n=0}^{N} t_n}. \tag{2.48}$$

Besides defining a "good" marker, it is important to select an appropriate reference realisation. We have done some investigations relative to this case and the results obtained are shown in Fig. 2.7. In one case the perturbation is kept constant while the system varies and in other case the system is kept constant.

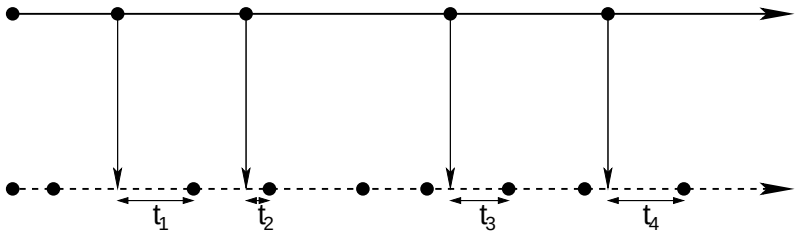

Figure 2.6: In this figure two realisations are shown. The full line represents the reference realisation. The intervals indicated by t_1, t_2, t_3 and t_4 are the *time differences*. Each dot represents an event. The time intervals between two consecutive events are laminar regions which are extracted from a Poisson distribution.

The result of Fig. 2.7 shows that there exists an influence of the P events on the occurrence times of the S events. In the absence of this influence, we would expect $R = 1$, the neutral condition. The condition $R < 1$ indicates that the time of occurrence of S events is closer to that of the P events than in the absence of coupling. This suggests that the P events attract the S events. The condition $R > 1$ indicates the opposite repulsion effect. If we keep g_S fixed and we increase g_P from values smaller to values larger than g_S (broken line in Fig. 2.7), we see the following: For $g_P < g_S$, $R > 1$ (repulsion condition). In the close proximity of $g_S = g_P$, R gets the values of 1, in the course of an almost abrupt transition to $R_{\min} < 1$, the attraction condition. The systems assumes this minimum value at $g_S = g_P$, and it maintains it in the whole region $g_P > g_S$. Analogously, if we keep g_P fixed, and we decrease g_S from values larger than g_P to values smaller (full line in Fig. 2.7), the parameter R moves from the condition $R > 1$, repulsion condition, to the neutral condition $R = 1$, in the close proximity of $g_P = g_S$, where it assumes the value $R_{\min}$, which is then maintained in the whole region $g_P < g_S$. A somewhat simplified description of all this is as follows. The rate matching condition $g_S = g_P$ is the border between the regime where the S events are attracted by the P events,

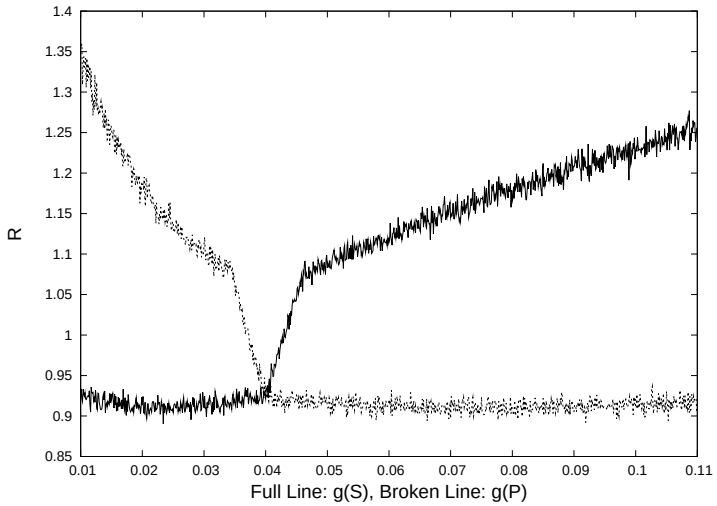

Figure 2.7: This figure shows the two cases that we examined: one in which g_S is kept constant (broken line) and the other where g_P is kept constant (full line). The broken-line curve reppresents the case where $g_S = 0.04$ is kept constant and the perturbation is taken as the reference realisation. The full-line curve reppresents the case where $g_P = 0.04$ is kept constant and the perturbation is taken as the reference realisation. In both cases the value of the perturbation strength is $\epsilon = 0.5$.

$g_S < g_P$, and the regime where the S events are repelled by the P events, $g_S > g_P$.

CHAPTER 3

Non-Poisson Systems

3.1 Background

In section 2.2 we dealt with a two-state system generating a stochastic processes with renewal. The evolution of such a process was reppresented by a two-state time series with events occurring at times t_i and separated by time intervals randomly selected from an exponential distribution. Each process was characterised by just one parameter, namely, the rate g at which the system switched between the two available states. We shall now consider a similar processes with the only difference that the time intervals are selected from an inverse-power probability distribution density. Such processes maintain the renewal property but are no longer Poissonian. Our goal is to study the power spectrum of non-Poisson processes generated from a waiting time distribution density of the form

$$\psi(\tau) = (\mu - 1)\frac{T^{\mu-1}}{(T+\tau)^{\mu}}, \tag{3.1}$$

where $1 < \mu < \infty$, keeping in mind that $\mu = 2$ is a special case in such a class. A theoretical study of such power spectra has already been done by the authors of Refs. [14, 36]. However, they do not emphasise on the case where $\mu = 2$. The function in Eq.(3.1) is a normalised probability density function. A closer inspection

shows that for $\mu > 2$, the first moment is given by

$$\langle \tau \rangle = \int_0^\infty \tau \psi(\tau') d\tau' = \frac{T}{\mu - 2}. \tag{3.2}$$

On the other hand, when $\mu < 2$, the function $\tau\psi(\tau)$ is not integrable and hence the average time interval does not exist. Stochastic processes with a waiting time distribution of the form shown in Eq.(3.1) can be divide into two groups: those with a finite first moment ($\mu > 2$) and those with no definite time scale ($\mu < 2$). The former are ergodic whilst the latter are not. Furthermore, the process with $\mu > 2$ are further divided into those with a finite second momentum, i.e. when $\mu > 3$ and those without one, i.e. when $2 < \mu < 3$. Right from the beginning we shall neglect processes with $\mu > 3$ since they all obey the central limit theorem and thus become Gaussian in the asymptotic limit.

Our decision to study a non-ergodic dichotomous processes with an inverse-power waiting time distribution was inspired by the results obtained in the study of colloidal nanocrystals or quantum dots. Under the right circumstances, such systems emit light intermittently, switching irregularly between bright and dark states [24]. Furthermore, the durations of these bright and dark periods follow an inverse-power distribution of the form

$$\psi(\tau) \propto \frac{1}{\tau^\mu}, \tag{3.3}$$

with $\mu < 2$ [25, 26]. This unexpected behaviour has also been observed in the fluorescence of single organic molecules [27, 28, 29, 30]. We used the power-law in the form shown in Eq.(3.1) purely out of practical reasons. The inclusion of the variable T, the time scale for which a power-law regime is reached, avoids problems at the origin ($\tau = 0$) when integrating. In the case of semiconductor nanocrystals the hypothesis was made that the time of sojourn in a given state, either "on" or "off", does not have any correlation with the other sojourn times [31]. This property, referred to as the *renewal* condition, has been confirmed by the careful statistical analysis of real data made by the authors of Ref. [32]. The renewal and the inverse power law condition with $\mu < 2$ generate *perennial aging* [34] and consequently a conflict with the ergodic assumption of statistical physics [35], thereby posing a challenge to the adoption of the prescriptions of ordinary statistical physics. Ergodicity breakdown has been recently observed also with the spectroscopy of single organic molecules

[37]. In the case of fluorescence blinking in nanocrystal quantum dots, the authors of Ref. [23, 38] found that these fluctuations have the spectral form of $1/f$ (flicker) noise. The phenomenon of flicker noise has been known for 82 years [39]. It describes the deviation of the noise spectral density from the flat condition, through the form

$$P(f) \propto \frac{1}{f^{\eta}}, \tag{3.4}$$

where f is the frequency and η ranges from $\eta = 0.5$ to $\eta = 1.5$. The authors of Refs. [23] and [38] found $\eta = 1.3$ and $\eta = 1.1$, respectively. In the literature of $1/f$ noise no attention has been devoted so far to the fact that, although $\eta < 1$ is compatible with the ergodic assumption, $\eta > 1$ [23, 38] may imply ergodicity breakdown, in spite of the fact that $\eta > 1$ is frequently found in the literature. In addition to $\eta > 1$ of Refs. [23, 38], see, for instance the flicker noise emerging from the scanning tunnelling microscopy [40] with $\eta \approx 1.08$.

The fact that the ergodic assumption is valid for $\eta < 1$ can be seen by adopting a very simple model made up of a collection of infinitely many independent linear oscillators [42]. The model shows that by assuming that the process in exam is ergodic we end up with a power spectrum having $\eta < 1$. The equation of motion of a single, one-dimensional harmonic oscillator with angular frequency ω is given by

$$x(t) = x(0)\cos(\omega t) + \frac{v(0)}{\omega}\sin(\omega t), \tag{3.5}$$

where $x(0)$ is the initial speed and $v(0)$ is the initial velocity. Alternatively, we can write

$$x(t) = A\cos(\omega t - \varphi), \tag{3.6}$$

where

$$A\cos(\omega t - \varphi) \equiv x(0)\cos(\omega t) + \frac{v(0)}{\omega}\sin(\omega t), \tag{3.7}$$

so that

$$A = \sqrt{x^2(0) + \frac{v^2(0)}{\omega^2}} \qquad \text{and} \qquad \tan\varphi = \frac{v(0)}{\omega x(0)}. \tag{3.8}$$

Consider now a very large amount of identical oscillators, all with the same angular frequency *omega*. A pair of initial conditions $x_i(0)$ and $v_i(0)$ is chosen randomly and assigned to each oscillator of the system. If they are allowed to interact, the system will reach an equilibrium state after some time if left on its own in the absence of external forces. An example of a large number of one-dimensional interacting oscillators is a very long chain of identical springs with identical masses attached to them. Imagine now that we somehow "freeze" the system together with all the oscillators in it. We can randomly extract a single oscillator and determine its displacement from the equilibrium position and the velocity it had just before being frozen. We can consider these quantities as being the initial conditions of the oscillator when we replace it and unfreeze the system. The probability, $p(x, v)dxdv$, that the randomly selected (frozen) oscillator has displacement $x \pm dx$ and velocity $v \pm dv$ is given by Boltzmann's theory. We consider the selected oscillator to be the system; all the others are part of the heat reservoir. In that case the probability density function is given by

$$p(x, v) = \frac{\omega m}{2\pi k_B T} \exp\left[-\frac{m}{2k_B T}\left(v^2 + \omega^2 x^2\right)\right], \tag{3.9}$$

where T is the temperature of the system. Therefore, we conclude that the initial conditions of all the oscillators placed together form a distribution equal to (3.9). In other words, the initial conditions of the oscillators are picked randomly from the distribution in (3.9). Consequently, the phase φ, and amplitude A in Eq. (3.6) are also random values. This random phase assumption is the key ingredient of the approach to $1/f$ noise proposed by Voss and Clarke [33]. According to the equipartition theorem, the mean energy of a single oscillator is given by

$$\left\langle \frac{1}{2}mv^2 + \frac{1}{2}m\omega^2 x^2 \right\rangle = \frac{1}{2}2k_B T = k_B T. \tag{3.10}$$

So far we have only considered oscillators with the same angular frequency, ω. Henceforth, we are going to explore a system composed of many oscillators with different frequencies. We follow Weiss [42] and assume that the frequency distribution is given by

$$c_j = c(\omega_j) = \omega_i^{\frac{\delta+1}{2}}. \tag{3.11}$$

This is an attractive way of going beyond ordinary statistical mechanics, or, using the terminology of Ref. [42], beyond the *ohmic* condition where $\delta = 1$. As we shall see bellow, it enables us to construct a stochastic process with a power spectrum that obeys the inverse power law. We create a fluctuation $\xi(t)$ by summing up the coordinates $x_i(t)$ of infinitely many linear harmonic oscillators:

$$\xi(t) = \sum_{j=0}^{M} \sum_{i=N_j}^{N_{j+1}} \left[x_i(0)\cos(\omega_j t) + \frac{v_i(0)}{\omega_j}\sin(\omega_j t) \right], \tag{3.12}$$

where

$$N_{j+1} - N_j = c(\omega_j) \quad \text{and} \quad c(\omega_j) \gg 1 \; \forall \; j. \tag{3.13}$$

We can also write Eq. (3.12) in the following form:

$$\xi(t) = \sum_{j=0}^{M} c_j \left[\tilde{x}_j(0)\cos(\omega_j t) + \frac{\tilde{v}_j(0)}{\omega_j}\sin(\omega_j t) \right], \tag{3.14}$$

where

$$\tilde{x}_j(0) = \frac{1}{N_{j+1} - N_j} \sum_{i=N_j}^{N_{j+1}} x_i(0),$$

$$\tilde{v}_j(0) = \frac{1}{N_{j+1} - N_j} \sum_{i=N_j}^{N_{j+1}} v_i(0).$$

The correlation function of the stochastic process $\xi(t)$ is given by

$$\langle \xi(t)\xi(t') \rangle = \sum_{j=0}^{M} c_j^2 \left[\langle \tilde{x}_j^2(0) \rangle \cos(\omega_j t)\cos(\omega_j t') + \frac{\langle \tilde{v}_j^2(0) \rangle}{\omega_j} \sin(\omega_j t)\sin(\omega_j t') \right] \tag{3.15}$$

We have omitted the mixed terms because the velocities and displacements are independent from one another and therefore

$$\langle x_j(0)v_j(0) \rangle = \langle x_j(0) \rangle \cdot \langle v_j(0) \rangle = 0. \tag{3.16}$$

Since the oscillators are independent, we also have that

$$\langle x_j(0)x_k(0)\rangle = 0 \quad \text{and} \quad \langle v_j(0)v_k(0)\rangle = 0 \quad \text{when} \quad j \neq k. \tag{3.17}$$

Again, according to the equipartition theorem, we have that

$$\langle v_j^2\rangle = \langle x_j^2\rangle\omega_j^2 = \frac{k_B T}{m}. \tag{3.18}$$

Consequently

$$\langle \xi(t)\xi(t')\rangle = \frac{k_B T}{m}\sum_{j=0}^{M}\frac{c_j^2}{\omega_j^2}\cos(\omega_j(t-t')). \tag{3.19}$$

By substituting (3.11) into (3.19), the normalised correlation function of $\xi(t)$ becomes

$$\Phi_\xi(t,t') \equiv \frac{\langle \xi(t)\xi(t')\rangle}{\langle \xi^2(t)\rangle} = \frac{\sum_{j=0}^{M}\omega_j^{\delta-1}\cos(\omega_j(t-t'))}{\sum_{j=0}^{M}\omega_j^{\delta-1}} = \frac{\sum_{j=0}^{M}\omega_j^{\delta-1}\cos(\omega_j\tau)}{\sum_{j=0}^{M}\omega_j^{\delta-1}}, \tag{3.20}$$

where $\tau = t - t'$. We have that

$$\lim_{\tau\to\infty}\Phi_\xi(\tau) \propto \frac{1}{t^\delta} \qquad \text{for} \qquad 0 < \delta < 1, \tag{3.21}$$

and

$$\lim_{\tau\to\infty}\Phi_\xi(\tau) \propto -\frac{1}{t^\delta} \qquad \text{for} \qquad 1 < \delta < 2. \tag{3.22}$$

Furthermore, Φ_ξ depends only on the time difference therefore it is a wide-sense stationary process. Consequently, it is enough to calculate the Fourier transform of Φ_ξ in order to obtain the power spectrum, $S(\omega)$ (Wiener-Khinchin theorem).

$$\widehat{\Phi}_\xi(\omega) = S(\omega) = A^{-1}\int_{-\infty}^{\infty}\sum_j \omega_j^{\delta-1}\cos(\omega_j\tau)e^{i\omega\tau}d\tau = A^{-1}\sum_j \omega_j^{\delta-1}\int_{-\infty}^{\infty}\cos(\omega_j\tau)e^{i\omega\tau}d\tau, \tag{3.23}$$

where $A = \sum_j \omega_j^{\delta-1}$ is a constant. Now,

$$\mathcal{F}\left[\cos(\omega_j\tau)\right] = \frac{1}{2}\mathcal{F}\left[e^{i\omega_j\tau} + e^{-i\omega_j\tau}\right] = \frac{1}{2}\left[2\pi\delta(\omega+\omega_j) + 2\pi\delta(\omega-\omega_j)\right]. \tag{3.24}$$

Before we precede with the evaluation of (3.23) we have to make a few assumptions. If we consider a reasonably large range of angular frequencies, ω_j, we can approximate the sum in (3.23) with an integral. Furthermore, there must be a lower and upper limit, so we write:

$$\sum_{j=0}^{j_{\mathrm{M}}} \longrightarrow \int_{\omega_0}^{\omega_{\mathrm{M}}} d\tilde{\omega}, \tag{3.25}$$

where $\omega_{\mathrm{M}} \gg \omega_0$ and $\omega_0 > 0$. In that case

$$S(\omega) = A^{-1}\pi \int_{\omega_0}^{\omega_{\mathrm{M}}} \tilde{\omega}^{\delta-1}\left[\delta(\omega+\tilde{\omega}) + \delta(\omega-\tilde{\omega})\right] d\tilde{\omega}. \tag{3.26}$$

Since the integration is performed over a positive set of values, the first term under the integral vanishes. Therefore,

$$S(\omega) \propto \frac{1}{\omega^{\eta}}, \quad \omega \in [\omega_0, \omega_{\mathrm{M}}], \tag{3.27}$$

where $\eta = 1 - \delta$. The case $\delta > 1$ does not yield $1/f$ noise so it is of no interest. Therefore, we only consider the case $0 < \delta < 1$ which corresponds to $0 < \eta < 1$. Note that $\delta = 1$ corresponds to white noise. In conclusion, the random phase model used by Voss and Clarke is adequate in explaining the $1/f$ behaviour of noise only in the case where $\eta < 1$. The adoption of a random phase resulted in a stationary correlation function. In the next section, we are going to study non-ergodic systems and in section 3.3 we will present a model that is compatible with both cases, $\eta < 1$ and $\eta > 2$. We shall see that the case $\eta > 1$ corresponds to the non-ergodic condition.

3.2 Theoretical Preliminaries

3.2.1 Non-Poisson Process

In the previous section, two important experimental results were mentioned: The fact that blinking quantum dots produce a time series that displays power-law statis-

tics with $\mu < 2$ and a power spectrum of the form $1/f^{\eta}$. Having these results in mind, we procede to uncover the entire picture by finding a relationship between μ and η.

We start by writing down the procedure for creating a single realisation or time series, $\xi(t)$, of a stochastic process that displays power-law statistics. Since we are considering only two-state systems, the time series will fluctuate between two values that are, in one way or another, related to the states of the system. The first thing to do is determine the length, L of the realisation. The next step is to identify the times at which the events of the stochastic process occur. We have already introduced the concept of events and collisions in section 2.1. In the case of blinking quantum dots there is no physical equivalent for events. Nevertheless, we shall use this concept because it is the only way we can directly link the waiting time distribution $\psi(\tau)$ to the autocorrelation function of the stochastic process [44]. What we actually see in the time series are the collisions and not the events. A collision is when there is a change of state, i.e. when the crystal either starts emitting light or ceases to do so. We always assume that an event occurs at time $t = 0$ and by doing so, we create what we call a prepared system. So, every time we start a realisation with an event, we intend that the system has been prepared. Having placed the first event at time $t = 0$, we randomly select a time interval τ_1 from the distribution in Eq.(3.1) and place an event at time $t = \tau_1$. We shall refer to the selected time intervals also as *laminar regions*. We then select another time interval, τ_2, randomly from $\psi(\tau)$ and place the second event at time $t = \tau_1 + \tau_2$. We continue in this way until we reach the end of the realisation, i.e. when $t = L$. Clearly, the final event will very rarely fall on the point $t = L$ so the interval between the last event and $t = L$ will not be equivalent to a time interval selected randomly from $\psi(\tau)$. The fact that we select a time interval (or laminar region), τ, randomly from a probability density function such as $\psi(\tau)$ creates renewal in the process. Renewal simply means that the time intervals are randomly selected from a distribution. The reason why we insist on using renewal events will be explained in subsection 3.2.2. As we have mentioned earlier, the stochastic process under study, $\xi(t)$, is related to a two-state system. We call the two states $|+\rangle$ and $|-\rangle$ and we assign the value $+1$ or -1 to $\xi(t)$ when the system is in the state $|+\rangle$ or $|-\rangle$ respectively. The final step is to assign one of the two possible values of $\xi(t)$ to each laminar region of the realisation. We do this by tossing a fair coin so that the values 1 and -1 are obtained with the same probability. For example, if we want to know what value to assign to the function

$\xi(t)$ in the interval between the first and second event, we simply have to toss a coin; if we get heads, we assign the value 1, if we get tails, we assign the value -1. In this way, we construct the collisions of the process. A collision coincides with an event that separates two neighbouring laminar regions with different values. Note that two or more consecutive laminar regions may share the same value. In the end, we obtain a time series characterised by the parameter μ from the waiting time distribution $\psi(\tau)$ in Eq.(3.1).

In the Poisson case, each stochastic process, and therefore system, was characterised by the rate, g, of event production. The difference between the $\xi(t)$ presented in this section and the $\xi(t)$ used in chapter 2 is that the laminar regions in the former case are extracted from

$$\psi(\tau) = (\mu - 1)\frac{T^{\mu-1}}{(T+\tau)^{\mu}} \qquad 1 < \mu < 3, \tag{3.28}$$

whilst the laminar regions in the later case are extracted from

$$\psi(\tau) = g\exp(-g\tau). \tag{3.29}$$

3.2.2 Aging

As we have already mentioned, the absence of a characteristic time scale in systems with $\mu < 2$ makes them non-ergodic, or following Bouchaud, *weakly non-ergodic* (see [35]). In the case of weak non-ergodicity, the system does visit all of its phase space but the fraction of time of occupation of a given volume in phase space is not equal to the fraction of phase space volume occupied by it. The specific systems that we are treating can only occupy one of two states at a time. Weakly non-ergodic means that globally, considering the total duration of the process, the system will spend more time in one state than it will in the other. If L is the total duration of the stochastic process, we would have

$$\lim_{L\to\infty}\int_0^L \xi(t)dt \neq 0. \tag{3.30}$$

We have seen in section 3.1 that systems with $\mu > 2$ have a characteristic time scale. Their mean sojourn time is given by the first moment of the waiting time distribution $\psi(\tau)$ (see Eq. (3.2)). Therefore, we can find an intermediate time interval such that

the time average and the ensemble average coincide. The fact is that all processes with renewal, governed by the inverse-power law in Eq.(3.1), undergo perennial aging (aging from now on). Processes with $\mu > 2$ become stationary and when they are infinitely aged. So, what is aging? Let us consider an ensemble of the realisations of $\xi(t)$, created in subsection 3.2.1 with the help of the waiting time distribution in Eq. (3.1). We shall assume that the realisations are infinitely long and, more importantly, that they are prepared at the origin, $t = 0$. At the moment, we shall not give importance to whether the first laminar regions are positive or negative. What is important is that there is an event at $t = 0$. If we set out to create a histogram using only the lengths of the first laminar regions of the realisations in the ensemble, it si obvious that we will end up with the waiting time distribution in (3.1),

$$\psi(\tau) = (\mu - 1)\frac{T^{\mu-1}}{(T+\tau)^{\mu}}. \tag{3.31}$$

After all, it is the waiting time distribution that we used to create each realisation. We shall refer to (3.31) as the infinitely young waiting time distribution. Now, we select a single realisation from the ensemble and move from the origin to an arbitrary position, $t = t_a$. It is possible that at $t = t_a$ there is an event. It is not important in which laminar region we find ourselves in or whether it is positive or negative. What is important is the absolute time, $t = t_a$. We move continuously from the position $t = t_a$ until we reach an event, say at some point $t = t^*$. We shall indicate with τ_{res} the distance between t_a and t^*, i.e. $\tau_{res} = t^* - t_a$. Of course, if at time $t = t_a$ there is an event, then $\tau_{res} = 0$. We calculate the residual time, τ_{res}, present in each realisation of the ensemble. Note that t_a is the same for each realisation. It is t^* that changes. If we plot a histogram with the residual times, we do not get the waiting time distribution in (3.31). What we get is a waiting time distribution of age t_a and we shall indicate it with ψ_{t_a}. The continuous change of the waiting time distribution from the time of preparation is an effect of aging. The analytical expression for the aged function is

$$\psi_{t_a}(\tau_{res}) = \sum_{n=0}^{\infty}\int_0^{t_a}\psi_n(t')\psi(t^*-t')dt' = \sum_{n=0}^{\infty}\int_0^{t_a}\psi_n(t')\psi(t_a+\tau_{res}-t')dt', \tag{3.32}$$

where $\psi_n(t')$ is the probability that the n^{th} event occurs in the time interval $[t', t' + dt']$. The function $\psi_{t_a}(t)$ is the probability of observing an event in the time interval $[t, t + dt]$ under the condition that the observation starts at $t = t_a$. When we start observing at $t = t_a$ we cannot know how many events had occurred. Since we are considering an ensemble, we have to include all the possibilities, from the case where no events occurred, to the case where infinite events occurred before $t = t_a$. This explains the presence of a sum in Eq. (3.32). The product $\psi_n(t')\psi(t^* - t')$ is the probability density that n events occurred before we started the observation and that that the first event after $t = t_a$ occurs at $t = t^*$. Although it is easy to explain Eq. (3.32) qualitatively, it is difficult to find an analytical expression if we substitute a waiting time distribution of the form shown in (3.31). The difficulty lies in finding an analytical expression for the event rate

$$P(t) = \sum_{n=0}^{\infty} \psi_n(t), \tag{3.33}$$

where

$$\psi_n(t) = \int_0^t \psi_{n-1}(\tau)\psi(t - \tau)d\tau. \tag{3.34}$$

Note that,

$$\psi_1(t) = \psi(t) \qquad \text{and} \qquad \psi_0(t) = \delta(t). \tag{3.35}$$

According to the authors of Ref. [18], a good approximation is to assume that $P(t)$ is constant when considering systems with a μ close to 2. They show that in the asymptotic limit $t \to \infty$,

$$P(t) = \frac{1}{\Gamma(2-\mu)\Gamma(\mu-1)} \frac{1}{T^{\mu-1}} \frac{1}{t^{2-\mu}}, \qquad \text{for} \qquad 1 < \mu < 2, \tag{3.36}$$

and

$$P(t) = \frac{\mu - 2}{T}\left[1 + \frac{T^{\mu-2}}{(3-\mu)} \frac{1}{t^{\mu-2}}\right] \qquad \text{for} \qquad 2 < \mu < 3. \tag{3.37}$$

We shall not provide a proof for the above statements since it is only a matter of mathematics. Details can be found in Ref. [19]. The infinitely young waiting

distribution that is used to create all the sequences in the ensemble is given by Eq. (3.31). We start from $t = 0$ and we let the ensemble evolve in time. After an amount of time t_a, the waiting time distribution becomes

$$\psi_{t_a}(\tau) = \int_0^{t_a} P(t)\psi(t_a + \tau - t)dt. \tag{3.38}$$

We assume that $P(t)$ is constant, thus

$$\psi_{t_a}(\tau) = \frac{1}{A(t_a)} \int_0^{t_a} \psi(t_a + \tau - t)dt = \frac{1}{A(t_a)} \int_0^{t_a} \psi(y + \tau)dy, \tag{3.39}$$

where $A(t_a)$ is the normalisation constant to be determined and $y = t_a - t$. The normalisation is given by

$$\begin{aligned} A(t_a) &= \int_0^{\infty} \psi(t, t_a)dt = \int_0^{\infty} dt \int_0^{t_a} \psi(t + y)dy = \int_0^{t_a} \int_0^{\infty} \psi(t + y)dt \\ &= \int_0^{t_a} dy \int_y^{\infty} \psi(t')dt' = \int_0^{t_a} \left(\frac{T}{T + y}\right)^{\mu-1} dy \\ &= \frac{T^{\mu-1}}{2 - \mu} \left[(T + t_a)^{2-\mu} - T^{2-\mu}\right]. \end{aligned}$$

The aged waiting time distribution is therefore

$$\psi_{t_a}(\tau) = (2 - \mu)\frac{(\tau + T)^{1-\mu} - (\tau + T + t_a)^{1-\mu}}{(T + t_a)^{2-\mu} - T^{2-\mu}}. \tag{3.40}$$

In the ergodic case ($2 < \mu < 3$), we see that for $t_a \to \infty$, the distribution $\psi_{t_a}(\tau)$ approaches a limiting value:

$$\lim_{t_a \to \infty} \psi_{t_a}(\tau) \equiv \psi_{\infty}(\tau) = (\mu - 2)\frac{T^{\mu-2}}{(T + \tau)^{\mu-1}}. \tag{3.41}$$

For $2 < \mu < 3$, the process evolves towards a stationary condition, where the survival probability is given by (3.41). For $1 < \mu < 2$, there is no limiting function, so the process does not tend to a stationary condition; the limit cannot be applied. Nevertheless, Eq. (3.40) is valid in the non-ergodic case ($1 < \mu < 2$) if we always consider finite values of t_a. In the limit for which $t_a \to 0$, and $2 < \mu < 3$, we obtain

the infinitely young distribution, $\psi(\tau)$:

$$\begin{aligned}\psi_{t_a}(\tau) &= (\mu-2)\frac{\dfrac{1}{(\tau+T)^{\mu-1}} - \dfrac{1}{(\tau+T)^{\mu-1}}\dfrac{1}{(1+t_a/(\tau+T))^{\mu-1}}}{\dfrac{1}{T^{\mu-2}} - \dfrac{1}{T^{\mu-2}}\dfrac{1}{(1+t_a/T)^{\mu-2}}} \\ &\simeq (\mu-2)\frac{\dfrac{1}{(\tau+T)^{\mu-1}} - \dfrac{1}{(\tau+T)^{\mu-1}}\left(1-(\mu-1)\dfrac{t_a}{(\tau+T)}\right)}{\dfrac{1}{T^{\mu-2}} - \dfrac{1}{T^{\mu-2}}\left(1-\dfrac{t_a}{T}(\mu-2)\right)} \\ &= (\mu-1)\frac{T^{\mu-1}}{(\tau+T)^{\mu}}. \end{aligned} \tag{3.42}$$

Similarly, when $1<\mu<2$, we have for $t_a \to 0$,

$$\begin{aligned}\psi_{t_a}(\tau) &\simeq (2-\mu)\frac{\dfrac{1}{(\tau+T)^{\mu-1}} - \dfrac{1}{(\tau+T)^{\mu-1}}\left(1-(\mu-1)\dfrac{t_a}{(\tau+T)}\right)}{T^{2-\mu}(1+(2-\mu)t_a/T) - T^{2-\mu}} \\ &= (\mu-1)\frac{T^{\mu-1}}{(\tau+T)^{\mu}}. \end{aligned} \tag{3.43}$$

Another important aspect of aging is the so-called *rejuvenation effect*. We consider Eq. (3.40) without considering the limit for which $t_a \to \infty$. Instead, we insist on the fact that the waiting time distribution is of the finite age t_a. We shall now study the two conditions: $\tau \ll t_a$ and $\tau \gg t_a$. We shall first consider the case where $\mu > 2$. When $\tau \ll t_a$, we rewrite Eq. (3.40) in the following form:

$$\begin{aligned}\psi_{t_a}(\tau) &= (2-\mu)\left[\frac{1}{(\tau+T)^{\mu-1}} - \frac{1}{(\tau+T+t_a)^{\mu-1}}\right]\left[\frac{1}{(T+t_a)^{\mu-2}} - \frac{1}{T^{\mu-2}}\right]^{-1} \\ &= (\mu-2)\frac{\left[\dfrac{1}{(\tau+T)^{\mu-1}} - \dfrac{1}{t_a^{\mu-1}((\tau+T)/t_a+1)^{\mu-1}}\right]}{\dfrac{1}{T^{\mu-2}} - \dfrac{1}{t_a^{\mu-2}}\dfrac{1}{(1+T/t_a)^{\mu-2}}} \\ &\simeq (\mu-2)\frac{1/(\tau+T)^{\mu-1}}{1/T^{\mu-2}} \\ &= (\mu-2)\frac{T^{\mu-2}}{(\tau+T)^{\mu-1}} \end{aligned} \tag{3.44}$$

This result coincides with Eq. (3.41), even though we have kept t_a finite. Observing only short sojourn times with respect to the age of the system makes it look much

older than it is. Under the other condition, $\tau \gg t_a$, therefore

$$\begin{aligned}\psi_{t_a}(\tau) &= (\mu-2)\frac{\dfrac{1}{(\tau+T)^{\mu-1}} - \dfrac{1}{(\tau+T)^{\mu-1}}\dfrac{1}{(1+t_a/(\tau+T))^{\mu-1}}}{\dfrac{1}{T^{\mu-2}} - \dfrac{1}{(T+t_a)^{\mu-2}}} \\ &\simeq (\mu-2)\frac{\dfrac{1}{(\tau+T)^{\mu-1}} - \dfrac{1}{(\tau+T)^{\mu-1}}\left(1-(\mu-1)\dfrac{t_a}{(\tau+T)}\right)}{1/T^{\mu-2}} \\ &= \frac{(\mu-2)t_a}{T}(\mu-1)\frac{T^{\mu-1}}{(\tau+T)^{\mu}}. \end{aligned} \tag{3.45}$$

This time, $\psi_{t_a}(\tau)$ is proportional to the infinitely young distribution, $\psi(\tau)$. This effect is called rejuvenation. The condition $\tau \gg t_a$ produces the opposite effect with respect to the condition $\tau \ll t_a$. Notice how the power index changes from $\mu - 1$ (infinitely aged condition) to μ (infinitely young condition). Aging implies that t_a is so large so as to make it impossible for us to observe sojourn times with a duration longer than t_a. In that case we are confined to $\tau \ll t_a$. This is when we observe aging. If $t_a < \infty$, both $\tau \ll t_a$ and $\tau \gg t_a$ are possible. The latter condition corresponds to rejuvenation. The former case corresponds to the infinitely aged state. If $t_a = \infty$, only the infinitely aged condition is possible. For $\mu < 2$, the results are very similar; the numerators in (3.44) and (3.45) remain the same. When $\tau \ll t_a$, then

$$\psi_{t_a}(\tau) \simeq (2-\mu)\frac{1/(\tau+T)^{\mu-1}}{(T+t_a)^{2-\mu} - T^{2-\mu}} \simeq \frac{(2-\mu)}{t_a^{2-\mu}}\frac{1}{(\tau+T)^{\mu-1}} \sim \frac{1}{\tau^{\mu-1}}. \tag{3.46}$$

On the other hand, when $\tau \gg t_a$,

$$\begin{aligned}\psi_{t_a}(\tau) &\simeq (2-\mu)(\mu-1)\frac{t_a/(\tau+T)^{\mu}}{(T+t_a)^{2-\mu} - T^{2-\mu}} \\ &\simeq (2-\mu)\frac{t_a^{\mu-1}}{T^{\mu-1}}\frac{(\mu-1)T^{\mu-1}}{(\tau+T)^{\mu}} \\ &= (2-\mu)\frac{t_a^{\mu-1}}{T^{\mu-1}}\psi(\tau) \\ &\propto \psi(\tau). \end{aligned} \tag{3.47}$$

We have very often stressed that the events used to create the realisations $\xi(t)$, must obey renewal. The reason for this is because a system, without the renewal property is not compatible with the aging theory presented above. Such systems

usually do not even experience aging, but when they do, the effect is only partial. For example, a stochastic process that is modulated by a deterministic prescription does not obey renewal. The authors of Ref. [20] found that under certain conditions, such systems experience aging, but only partially. This explains why we are interested in processes with renewal; they experience the aging process completely.

We now want to show that a process that is characterised by Poisson-statistics does not experience aging. We use the dichotomous realisations $\xi(t)$ introduced in section 2.2. In that case, we have that the waiting time distribution is given by

$$\psi(\tau) = g\exp(-g\tau), \tag{3.48}$$

where g is the rate of the events in the Poisson process. All we have to do is substitute (3.48) into Eq. (3.32). Before we continue, we have to calculate $P(t)$. The simplest method is to use the Laplace-transform of $\psi_n(t)$ (we use the tilde to indicate the Laplace transform):

$$\tilde{\psi}_n(u) = \tilde{\psi}_{n-1}(u)\tilde{\psi}_1(u) = \left[\tilde{\psi}(u)\right]^n = \left(\frac{g}{g+u}\right)^n. \tag{3.49}$$

Anti-transforming, we obtain

$$\psi_n(t) = (gt)^{n-1}\frac{ge^{-gt}}{(n-1)!}. \tag{3.50}$$

We can now calculate the aged waiting time distribution in the Poisson case:

$$\begin{aligned}
\psi_{t_a}(t) &= \psi(t) + \sum_{n=1}^{\infty}\int_0^{t_a}\psi_n(t')\psi(t-t')dt' \\
&= g\exp(-gt) + g^2\sum_{n=1}^{\infty}\int_0^{t_a}\frac{(gt')^{n-1}}{(n-1)!}\exp(-gt')\exp(-g(t-t'))dt' \\
&= g\exp(-gt) + g^2\exp(-gt)\int_0^{t_a}\sum_{n'=0}^{\infty}\frac{(gt')^{n'}}{n'!}dt' \\
&= g\exp(-gt) + g^2\exp(-gt)\int_0^{t_a}\exp(gt')dt' \\
&= g\exp[-g(t-t_a)].
\end{aligned} \tag{3.51}$$

In the Poisson case

$$\psi_{t_a}(\tau_{res}) = \psi_{t_a}(t) = \psi(t - t_a) = \psi(\tau_{res}). \tag{3.52}$$

The waiting time distribution remains the same. Aging has been studied extensively in the literature. See, for example, Refs. [16, 17, 21] for more details. We have introduced the concept of aging because we shall need it shortly, when we investigate the autocorrelation functions of non-ergodic processes. What we have said so far regarding aging should be enough for such a task.

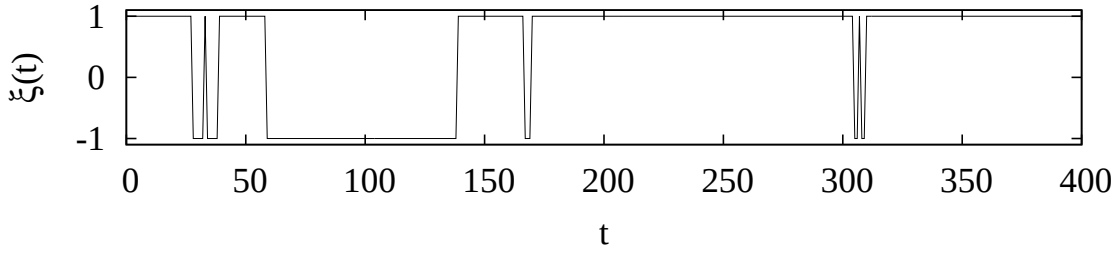

Figure 3.1: A typical time series or realisation. The function $\xi(t)$ fluctuates between the two values $+1$ and -1.

3.2.3 Autocorrelation

By definition, the autocorrelation function of a stochastic process $\xi(t)$ is

$$\Phi_\xi(\tau; t) = \langle \xi(t)\xi(t+\tau) \rangle, \tag{3.53}$$

where $\langle \ldots \rangle$ denotes an ensemble average. This definition is applicable to both, stationary and non-Stationary-stationary processes. If the process is stationary, then Φ_ξ is independent of the time t. An ensemble average means that we have to use an infinite number of realisations of the stochastic process $\xi(t)$.

Let us consider a Gibbs ensemble of prepared sequences, $\xi(t)$, with an arbitrary μ. All the sequences are prepared so that at $t = 0$ there is an event and all of them begin with a positive laminar region, i.e. $\xi(t) = +1$ for $0 \leq t \leq \tau_1$. By definition, the Gibbs average of $\xi(t)$ is given by

$$\langle \xi(t) \rangle = \lim_{N \to \infty} \frac{1}{N} \sum_{n=1}^{N} \xi_n(t), \tag{3.54}$$

where $\xi_n(t)$ is the n^{th} realisation of the ensemble. By construction, we have that $\langle\xi(0)\rangle = 1$. We now argue that the function $\langle\xi(t)\rangle$ will decay in the same way in which its corresponding survival probability decays. In other words

$$\langle\xi(t)\rangle = \Psi(t) = \int_t^\infty \psi(t')dt'. \tag{3.55}$$

A more rigorous demonstration can be found in Ref. [17]. A sequence chosen randomly from the ensemble will have the first laminar region positive. Let us imagine that its second laminar region is also positive and that the first laminar region is of length τ_1 and the second τ_2. Since there is an infinite number of realisations, there are surely others whose first two laminar regions are also of length τ_1 and τ_2. Moreover, we are using the coin tossing method to decide the value of ξ in every laminar region apart from the first. Therefore half of the second laminar regions of length τ_2 will be positive and half will be negative. When we sum up these realisations, the second laminar regions will cancel each other out. This argument can be applied to all the other sequences. If we sum all the realisations present in the ensemble and normalise, we end up with the ensemble average of $\xi(t)$. It is obvious that $\langle\xi(t)\rangle$ is a decaying function of time, after all, the first laminar region is always positive. What is less obvious is that $\langle\xi(t)\rangle$ decays as the survival probability, $\Psi(\tau)$,

$$\Psi(\tau) = \int_\tau^\infty \psi(t)dt. \tag{3.56}$$

This is because all the first laminar regions survive after the summation and the second laminar regions cancel each other out. The surviving laminar regions are distributed according to the waiting time distribution and therefore add up to form the survival probability function. We can now use Eq. (3.53) to calculate the autocorrelation function for $t = 0$. We have

$$\Phi_\xi(\tau; t = 0) = \langle\xi(0)\xi(\tau)\rangle. \tag{3.57}$$

But, we know that at $t = 0$, the realisation is always positive, therefore

$$\Phi_\xi(\tau; 0) = \langle\xi(\tau)\rangle = \Psi(\tau). \tag{3.58}$$

Note that the method we used to derive the autocorrelation function rests on the

assumption that the events in $\xi(t)$ are generated with the renewal property.

Stochastic processes with $\mu < 2$ are always non-stationary and therefore their correlation functions change with time. The correlation function changes due to the aging process [17]. We can use an argument similar to the one above and calculate the correlation function at any time $t = t_a$. We prepare the ensemble in such a way that at $t = 0$ half of the realisations are positive and half are negative. This produces a vanishing mean at the origin, $\langle \xi(t = 0) \rangle = 0$. Nevertheless, at $t = 0$, the ensemble is non-stationary and it is not . Then, we let the ensemble evolve up to time $t = t_a$. At this time we select all the sequences characterised by $\xi(t_a) = 1$. The sum over all these realisations corresponds to a macroscopic out-of-equilibrium fluctuation whose value is M, with $M \approx N/2$ and N is the total number of realisations. In this case, $\langle \xi(t_a) \rangle = 1$ and the Gibbs average regresses slowly to zero. We again evoke the property of the coin-tossing procedure and the fact that the ensemble was prepared at $t = 0$ in order to determine the autocorrelation function. The fact that we prepared the ensemble implies that the residues $\tau_{res} = t^* - t_a$ are distributed according to the aged waiting time distribution $\psi_{t_a}(\tau_{res})$. The fact that we used the coin-tossing method implies that the laminar regions that start at $t = t^*$ will vanish during the summation process. Consequently, if we move the origin to $t = t_a$ and forget about what happend before this time, we can conclude that

$$\langle \xi(t) \rangle = \Psi_{t_a}(t) = \int_t^\infty \psi_{t_a}(t')dt'. \tag{3.59}$$

By construction, $\xi(t_a) = 1$, therefore we can easily determine the autocorrelation function. In fact,

$$\Phi_\xi(\tau; t_a) = \langle \xi(t_a)\xi(t_a + \tau) \rangle = \langle \xi(t_a + \tau) \rangle = \langle \xi(\tau) \rangle = \Psi_{t_a}(\tau). \tag{3.60}$$

According to the results obtained above, a process with $\mu > 2$ that is stationary will have the correlation function,

$$\Phi(\tau) = \Psi_\infty(\tau). \tag{3.61}$$

This is because a prepared sequence, having $\mu > 2$, becomes stationary only after it has evolved for an infinite time. In that case, $t_a = \infty$ and the autocorrelation function is equal to the infinitely aged survival probability. In a way, $\Psi_\infty(\tau)$ is

the limiting autocorrelation function. At $t = 0$, $\Phi_\xi(\tau) = \Psi(\tau)$. As time passes the autocorrelation evolves and tends towards the limit $\Psi_\infty(\tau)$. When $\mu < 2$, the process never approaches a stationary condition, so the autocorrelation keeps on changing, without approaching a limiting function. In conclusion, we have found shown that the use of the coin-tossing procedure generates an autocorrelation function that is related to the waiting time distribution through Eqs. (3.59) and (3.60). This is the reason why in section 2.1 (see Eq. (2.8)) we decided to use the rate $g = 2q$ instead of just the Kramers rate, q. If we apply the results of this section, then the autocorrelation function of a Poisson process with a rate g, using the coin-tossing procedure, is given by

$$\Phi_\xi(\tau) = \Psi(\tau) = \int_\tau^\infty g \exp(-g\tau) = \exp(-g\tau). \tag{3.62}$$

On the other hand, the autocorrelation function of a Poisson process with the Kramers rate q, without the coin-tossing procedure, is given by

$$C_\xi(\tau) = \exp(-2q\tau). \tag{3.63}$$

Since the two methods have to produce the same realisation $\xi(t)$, then comparing $C_\xi(\tau)$ with $\Psi_\xi(\tau)$ we conclude that $g = 2q$. We now give a proof for the statement in Eq. (3.63). A Poisson process is characterised by a waiting time distribution of the form

$$\psi(\tau) = q \exp(-q\tau). \tag{3.64}$$

The rate of events is given by $P(t)$ in Eq. (3.33), whose Laplace transform is

$$\tilde{P}(u) = \int_0^\infty \exp(-ut)P(t)dt = \sum_{n=0}^\infty \tilde{\psi}_n(u) = \sum_{n=0}^\infty \Big(\tilde{\psi}(u)\Big)^n = \frac{1}{1-\tilde{\psi}(u)}. \tag{3.65}$$

Since

$$\tilde{\psi}(u) = q\int_0^\infty \exp(-ut)\exp(-qt)dt = \frac{q+u}{q}, \tag{3.66}$$

we have that the anti-transform of $\tilde{P}(u)$ gives

$$P(t) = 2\delta(t) + q. \tag{3.67}$$

Therefore in the Poisson case, the rate is constant apart from the singularity in zero. If we consider a two-state system with a waiting time distribution given by Eq. (3.64), then the rate at which the system switches between states is q. Let us assume that the two states are $|+\rangle$ and $|-\rangle$. As the system evolves in time, it will produce an output signal $\xi(t)$ which is related to the state occupied by the system at time t. When the system is in the state $|+\rangle$ the output signal $\xi(t)$ will have the value $+1$ and when it is in $|-\rangle$, ξ will have the value -1. The evolution of such a process can be described by the master equation,

$$\begin{aligned}\frac{d}{dt}P_{|+\rangle}(t) &= -qP_{|+\rangle}(t) + qP_{|-\rangle}(t)\\ \frac{d}{dt}P_{|-\rangle}(t) &= -qP_{|-\rangle}(t) + qP_{|+\rangle}(t),\end{aligned} \tag{3.68}$$

where $P_{|\pm\rangle}$ is the probability of finding the system in the state $|\pm\rangle$. We introduce the variable

$$\langle\xi(t)\rangle = \Pi(t) = P_{|+\rangle}(t) - P_{|-\rangle}(t).$$

Substituting into (3.68), yields

$$\dot{\Pi}(t) = -2q\Pi(t). \tag{3.69}$$

Integrating, we get

$$\Pi(t) = \Pi(0)\exp(-2qt). \tag{3.70}$$

If consider an ensemble of systems, and place all of them in the state $|+\rangle$ at $t = 0$, then $P(0) = 1$ and the mean value becomes

$$\langle\xi(t)\rangle = \exp(-2qt). \tag{3.71}$$

Since the rate is constant, we have a stationary process and the autocorrelation

function is given by

$$C_\xi(t) \equiv \langle \xi(t+\tau)\xi(t)\rangle = \langle \xi(\tau)\rangle = \exp(-2q\tau). \tag{3.72}$$

3.2.4 Power Spectrum of a Stationary Process

In the previous subsection we saw that processes with $\mu > 2$ are stationary if they are not prepared. The advantage of dealing with stationary processes is that we can apply the Wiener-Khinchin theorem in order to obtain the power spectrum. To do so, we first have to find the corresponding autocorrelation function. In the previous subsection we used a Gibbs ensemble of realisations and found that the correlation function of an infinitely long realisation with $\mu > 2$ is equal to its infinitely aged survival probability function (see for example Ref. [17] for details). In other words, if $\psi(\tau)$ is the waiting time distribution, then the correlation function is

$$\Phi_\xi(\tau) = \Psi_\infty(\tau) \equiv \int_\tau^\infty \psi(t)dt. \tag{3.73}$$

We are going to show that the same result can be obtained by using only one realisation of $\xi(t)$. Let us assume that we are given a single realisation of $\xi(t)$, infinite in length. Then, by definition, the correlation function is

$$\Phi_\xi(\tau) \equiv \lim_{L\to\infty} \frac{1}{L}\int_0^{L-\tau} \xi(t)\xi(t+\tau)dt. \tag{3.74}$$

Eq. (3.74) obtained by moving a window of length τ along the entire realisation $\xi(t)$. If we adopt the coin-tossing method described earlier we can use the following expression (see Ref. [15]):

$$\Phi_\xi(\tau) = \frac{1}{\langle\tau\rangle}\int_\tau^\infty d\tau' \frac{(\tau'-\tau)}{\tau'}\tau'\psi(\tau'), \tag{3.75}$$

where $\psi(t)$ is the waiting time distribution density used to create the process $\xi(t)$ and $\langle\tau\rangle$ is the mean laminar region. We still use the method whereby a window of length τ is moved along the entire realisation. Since the realisation was prepared by the coin-tossing procedure, the only situations that contribute to the correlation function are those in which the window falls entirely within a laminar region. In that case the contribution is always positive, no matter what sign was attributed

to the laminar region. If the window has its two ends in different laminar regions, then it will either give a positive contribution or a negative one. Since the process is stationary, for every positive contribution to the correlation function, there will be a negative one, thereby providing a vanishing average contribution.

In order to explain Eq. (3.75) let us assume that we have a realisation of length L, with N laminar regions, both N and L being very large numbers. The realisation will on average accommodate $N\psi(\tau')d\tau'$ laminar regions that have a length between τ' and $\tau' + d\tau'$. The same laminar regions will therefore occupy a time space equal to $\tau' \cdot N\psi(\tau')d\tau'$ which is only a fraction of the total time L, the length of the entire realisation. So, the fraction of the realisation occupied by laminar regions of length τ' is given by

$$\frac{N}{L}\tau'\psi(\tau')d\tau'. \tag{3.76}$$

However, (3.76) is also the probability that the starting point of the window falls into a laminar region of length τ'. If we take the limit for which $L \to \infty$, consequently $N \to \infty$ and we have that $N/L \to 1/\langle\tau\rangle$. The term $(\tau' - \tau)/\tau'$ is just the probability that the other end of the window remains in the same laminar region.

We procede by simplifying (3.75),

$$\begin{aligned}
\Phi_\xi(\tau) &= \frac{1}{\langle\tau\rangle}\int_\tau^\infty d\tau'(\tau'-\tau)\psi(\tau') \\
&= \frac{1}{\langle\tau\rangle}\left[\int_0^\infty d\tau'(\tau'-\tau)\psi(\tau') - \int_0^\tau d\tau'(\tau'-\tau)\psi(\tau')\right] \\
&= \frac{1}{\langle\tau\rangle}\left[\langle\tau\rangle - \tau - \int_0^\tau d\tau'(\tau'-\tau)\psi(\tau')\right] \\
&= 1 - \frac{\tau}{\langle\tau\rangle} - \frac{1}{\langle\tau\rangle}\int_0^\tau d\tau'(\tau'-\tau)\psi(\tau').
\end{aligned} \tag{3.77}$$

When we derive both sides of Eq. (3.77), we get

$$\Phi'_\xi(\tau) = -\frac{1}{\langle\tau\rangle} + \frac{1}{\langle\tau\rangle}\int_0^\tau d\tau'\psi(\tau'). \tag{3.78}$$

Deriving a second time produces

$$\Phi''_{\xi}(\tau) = \frac{1}{\langle\tau\rangle}\psi(\tau). \tag{3.79}$$

The infinitely aged case of the waiting time distribution $\psi(\tau)$ is given by [16]

$$\psi_{\infty}(\tau) = \frac{1}{\langle\tau\rangle}\int_{\tau}^{\infty}\psi(t')dt', \tag{3.80}$$

where

$$\langle\tau\rangle = \int_{0}^{\infty}\tau\psi(\tau)d\tau. \tag{3.81}$$

Furthermore, the survival probability that corresponds to $\psi_{\infty}(\tau)$ is

$$\Psi_{\infty}(\tau) = \int_{\tau}^{\infty}\psi_{\infty}(t')dt' = \int_{\tau}^{\infty}dt'\frac{1}{\langle\tau\rangle}\int_{t'}^{\infty}\psi(t'')dt''. \tag{3.82}$$

From Eq. (3.79) we see that $\psi(\tau) = \langle\tau\rangle\Phi''_{\xi}$. By substituting this value into the above equation, we see that [17]

$$\Psi_{\infty}(\tau) = \Phi_{\xi}(\tau). \tag{3.83}$$

For $\mu > 2$ we have that the survival probability of the infinitely aged waiting time distribution is equal to the correlation function (see Eq.(3.41)):

$$\Phi_{\xi}^{(\infty)} = \int_{\tau}^{\infty}\psi_{\infty}(t)dt = (\mu-2)\int_{\tau}^{\infty}\frac{T^{\mu-2}}{(t+T)^{\mu-1}}dt = \left(\frac{T}{T+\tau}\right)^{\mu-2}. \tag{3.84}$$

At this point we can use the Wiener-Khinchin theorem together with the correlation function in Eq. (3.84) in order to calculate the power spectrum of a stationary process with $\mu > 2$. Accordingly, we have

$$S(\omega) = 2\int_{0}^{\infty}\left(\frac{T}{T+\tau}\right)^{\mu-2}\cos(\omega\tau)d\tau = 2T^{\mu-2}\int_{0}^{\infty}(T+\tau)^{2-\mu}\cos(\omega\tau)d\tau. \tag{3.85}$$

Using the substitution $x = T + \tau$,

$$S(\omega) = 2T^{\mu-2}\int_{T}^{\infty}x^{2-\mu}\cos[\omega(x-T)]dx. \tag{3.86}$$

Another substitution, $y = \omega x$ gives

$$\begin{aligned} S(\omega) &= 2T^{\mu-2} \int_{\omega T}^{\infty} \left(\frac{y}{\omega}\right)^{2-\mu} \cos(y - \omega T) \frac{dy}{\omega} \\ &= \frac{2T^{\mu-2}}{\omega^{3-\mu}} \left[\cos(\omega T) \int_{\omega T}^{\infty} y^{2-\mu} \cos(y) dy + \sin(\omega T) \int_{\omega T}^{\infty} y^{2-\mu} \sin(y) dy\right] \end{aligned} \tag{3.87}$$

Since we are interested in very low frequencies, we assume that $\omega T \ll 1$. Consequently $\cos(\omega T) \approx 1$ and $\sin(\omega T) \approx \omega T$ and

$$S(\omega) = \frac{2T^{\mu-2}}{\omega^{3-\mu}} \left[\int_{\omega T}^{\infty} y^{2-\mu} \cos(y) dy + \omega T \int_{\omega T}^{\infty} y^{2-\mu} \sin(y) dy\right]. \tag{3.88}$$

For frequencies below $1/T$, it is the first term that dominates and hence the second term can be neglected. We compare the frequencies to $1/T$ because the value of T corresponds to the time it takes for the process to enter the regime of power-law statistics. Times the are shorter than T do not obey the $1/\tau^{\mu}$ power-law. This is why we are only interested in frequencies below $\omega = 1/T$. Finally, we have

$$S(\omega) = \frac{2T^{\mu-2}}{\omega^{3-\mu}} A(\mu, \omega) \sim \frac{1}{\omega^{3-\mu}} \propto \frac{1}{f^{3-\mu}}, \tag{3.89}$$

where

$$A(\mu, \omega) = \int_{\omega T}^{\infty} y^{2-\mu} \cos(y) dy \tag{3.90}$$

is a very slow function of ω. As expected, Eq.(3.89) is in accordance with the experimental result shown in Eq.(3.4); it is enough to link the two equations using the equality $\eta = 3 - \mu$, where $\mu \gtrsim 2$. Alternatively, if we neglect T, then (3.85) becomes

$$S(\omega) = 2 \int_{0}^{\infty} \tau^{2-\mu} \cos(\omega\tau) d\tau. \tag{3.91}$$

Neglecting T means that the process immediately acquires power-law statistics. For $2 < \mu < 3$, the integral in (3.91) can be solved without introducing any truncations in order to avoid problems at the origin. In fact the standard Fourier cosine transform

tables (see [43]) show that

$$2\int_0^\infty \tau^{2-\mu}\cos(\omega\tau)d\tau = \frac{\pi}{\Gamma(\mu-2)}\sec\left[\frac{\pi}{2}(\mu-2)\right]\omega^{\mu-3}, \tag{3.92}$$

for $\omega > 0$ and $2 < \mu < 3$. In the next section we shall investigate the power-spectra of non-stationary processes.

3.3 Power-Spectrum of Non-Poisson Systems

Our main purpose in this section is to study the properties of power-spectra produced by the non-Poisson two-state systems introduced previously. Each system, therefore, produces a finite dichotomous time series $\xi(t)$, characterised by the parameter μ ($1 < \mu < 3$). The choice of using a finite time series brings us closer to the real experimental conditions, allowing us to compare our numerical results with experimental results obtained by other authors. The power spectra of the non-ergodic case ($1 < \mu < 2$) have already been studied by Zumofen and Klafter [14]. However, they considered a truncated waiting time distribution. This means that the distance between two consecutive events in the time series cannot be greater then some predetermined maximum value, T_{max}. Truncating the waiting time distribution renders it integrable and consequently introduces a well defined time scale, or first moment. In such cases, ergodicity is maintained and the aging process is altered. The waiting time distribution tends to a limiting function just like in the ergodic case, where $\mu > 2$. Under such conditions, they were able to develop a theory for $\mu < 2$ by using the arguments that we presented in subsection 3.2.4. We, on the other hand consider the entire waiting time distribution ($T_{max} = \infty$) and use a generalised form of the Wiener-Khinchin theorem, compatible with the ergodicity breaking condition. Such a generalisation has been attempted by Margolin and Barkai [36]. These authors proposed a generalisation of the Wiener-Khinchin theorem that does not require the adoption of averages over the Gibbs ensemble. We provide a slightly different theoretical approach, placing our results in the context of $1/f$-noise. The ideal $1/f$ condition is a singularity corresponding to $\mu = 2$, the boarder between ergodicity ($\mu > 2$) and non-ergodicity ($\mu < 2$). Furthermore, we use autocorrelation functions obtained by adopting a Gibbs ensemble, subsection 3.2.3. We shall first present the numerical results and then, in a separate subsection, interpret them using the theoretical tools discussed in section 3.2.

We define the power spectrum, $S(\omega)$, of the time series in the usual way (see [14]) but without considering the limit $L \to \infty$:

$$S(\omega) = \frac{1}{L}\hat{\xi}(\omega)\hat{\xi}^*(\omega) = \frac{1}{L}|\hat{\xi}(\omega)|^2, \tag{3.93}$$

where L is the duration of the time series and $\hat{\xi}(\omega)$ is the Fourier-transform of $\xi(t)$; to be precise,

$$\hat{\xi}(\omega) = \mathcal{F}[\xi(t)] \equiv \int_{-\infty}^{\infty} \xi(t) e^{i\omega t} dt. \tag{3.94}$$

Since we are dealing with stochastic processes, the events observed in the time series occur randomly and therefore it is not possible to calculate the Fourier-transform of $\xi(t)$ analytically. At some point we have to make use of the computer. Fortunately, $\xi(t)$ has a very simple form, so the integral in Eq.(3.94) can be broken down into sums:

$$\hat{\xi}(\omega) = \sum_{n=0}^{N} \int_{t_n}^{t_{n+1}} \xi(t) e^{i\omega t} dt, \tag{3.95}$$

where t_n is the time of occurrence of the n^{th} event and $\xi(t)$ alternates between 1 and -1. Each integral in the sum is very easy to solve explicitly. The general case is

$$\begin{aligned} I[a,b] = \int_a^b e^{i\omega t} dt &= -\frac{i}{\omega}\left[e^{i\omega b} - e^{i\omega a}\right] \\ &= -\frac{i}{\omega}\left[\cos(\omega b) + i\sin(\omega b) - \cos(\omega a) - i\sin(\omega a)\right] \\ &= \frac{1}{\omega}\left[-i\cos(\omega b) + \sin(\omega b) + i\cos(\omega a) - \sin(\omega a)\right] \\ &= \frac{1}{\omega}\left[\sin(\omega b) - \sin(\omega a) + i\{\cos(\omega a) - \cos(\omega b)\}\right] \\ &= \frac{-\sin(\omega a) + \sin(\omega b)}{\omega} + i\frac{\cos(\omega a) - \cos(\omega b)}{\omega}, \end{aligned}$$

where a and b are two random numbers and $a < b$. Eq.(3.95) can be rewritten in the form:

$$\hat{\xi}(\omega) = \sum_{n=0}^{N} (\pm)_n I[t_n, t_{n+1}], \tag{3.96}$$

where $(\pm)_n$ is the value of $\xi(t)$ in the time interval $[t_n, t_{n+1}]$. The time series is dichotomous and we assume that $\xi(t)$ can either be $+1$ or -1. Consequently, $(\pm)_n$ is a random variable whose outcome can be either $+1$ or -1, with the same probability. This is true for every n apart from $n = 0$. We prepare the realisation so that $(\pm)_0 = 1$ always. Given that the time series is of length L, the explicit expression for the Fourier-transform of $\xi(t)$ is

$$\hat{\xi}(\omega) = \frac{1}{\omega}\sum_{n=0}^{N-1}(\pm)_n\left[-\sin(\omega t_n) + \sin(\omega t_{n+1})\right] + \frac{(\pm)_N}{\omega}\left[-\sin(\omega t_N) + \sin(\omega L)\right]$$
$$+i\frac{1}{\omega}\sum_{n=0}^{N-1}(\pm)_n\left[\cos(\omega t_n) - \cos(\omega t_{n+1})\right] + i\frac{(\pm)_N}{\omega}\left[\cos(\omega t_N) - \cos(\omega L)\right]. \tag{3.97}$$

We use a computer to generate the random time intervals (laminar regions), $\tau_{n+1} = t_{n+1} - t_n$, of $\xi(t)$. Each laminar region is extracted randomly from the waiting time distribution

$$\psi(\tau) = (\mu - 1)\frac{T^{\mu-1}}{(T+\tau)^{\mu}}. \tag{3.98}$$

Note that

$$t_n = \tau_1 + \tau_2 + \ldots + \tau_n = t_{n-1} + \tau_n, \tag{3.99}$$

where $t_0 = 0$. The computer therefore generates the random time intervals and uses (3.99) to calculate the sum in Eq. (3.97). $\xi(t)$ is a real function and it is not symmetric, therefore its Fourier-transform will be a complex number,

$$\hat{\xi}(\omega) = \hat{\alpha}(\omega) + i\hat{\beta}(\omega). \tag{3.100}$$

The final step is for the computer to determine the value of

$$S(\omega) = \frac{1}{L}|\hat{\xi}(\omega)|^2 = \frac{1}{L}\left[\hat{\alpha}^2(\omega) + \hat{\beta}^2(\omega)\right]. \tag{3.101}$$

3.3.1 Numerical Results

Fig.(3.2) is our first important numerical result. It shows that the power spectrum does indeed obey the inverse-power law expressed in Eq.(3.4) for a range of values of μ close to 2. It confirms the numerical and theoretical results of Margolin and Barkai [35], although, they considered only the case where $1 < \mu < 2$. As we have said earlier, the value of T in the waiting time distribution (Eq.(3.1)) gives us an indication of how long it takes for the system to enter into the regime of power-law statistics. We are therefore interested only in time scales larger than T. This is the reason why we shall study the power spectra for $\omega \ll 1/T$. Following Pelton et al. [23], we compare the power spectrum of an ensemble of realisations to that of a single realisation. Fig.(3.3) shows that the inverse-power law is maintained even at the level of a single realisation, thus confirming the experimental results obtained by the authors of [23]. The adoption of an ensemble merely reduces the noise and this can be seen in Fig.(3.5) where 1000 realisations were employed. Figs. (3.4) and (3.5) show the effect that the length of the realisation has on systems with $\mu > 2$ and $\mu < 2$ respectively. In both cases, we are dealing with non-stationary systems with the difference that those with $\mu > 2$ become stationary as $L \to \infty$ whilst those with $\mu < 2$ always remain non-stationary. When $\mu > 2$ the power spectrum does not depend significantly on the length of the realisation even though the process is non-stationary for small values of L. On the other hand, when $\mu < 2$, there is a strict dependence on the realisation length; the power spectrum decreases in intensity as the length is increased. The exact dependence on L is shown in Fig.(3.8). Introducing a cutoff in the waiting time distribution, $\psi(\tau)$, so that time intervals greater than some upper limit T_{max} are never present in the realisation produces notable effects on the power spectrum. First of all, a plateau is created for frequencies under $1/T_{max}$ and this can be seen in Fig.(3.6). Secondly, the power spectrum becomes independent of L when the realisation is greater than T_{max}; see Figs. (3.7) and (3.8). Zumofen and Klafter studied the power spectra of systems characterised by a truncated waiting time distribution in their 1993 paper, [14]. We, on the other hand, are going to present an argument that explains the behaviour of power spectra of systems with $T_{max} = \infty$.

For completeness, we calculated the power spectrum also for large values of ω. By large values, we intend $\omega > 1/T$. Fig. (3.9) shows the power spectrum for a very large range of frequencies. We can see that there is a change in regime somewhere

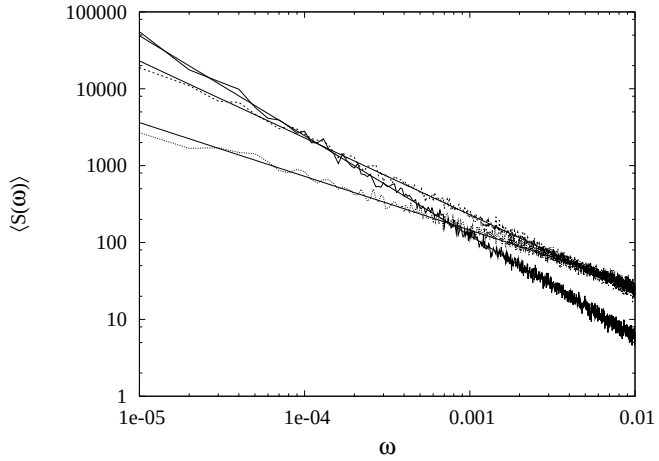

Figure 3.2: COMPARISON OF POWER SPECTRA OF SYSTEMS WITH DIFFERENT μ. Each curve was obtained by using an ensemble of 100 realisations of length $L = 10^6$ time units. The curves reppresent the power-spectra of processes with $\mu = 2.3$ (dotted curve), $\mu = 2.0$ (dashed curve) and $\mu = 1.7$ (full curve). The straight lines are the corresponding fits: $1.15\omega^{-0.7}$, $0.23\omega^{-1}$, $0.0155\omega^{-1.3}$.

around $\omega = 1/T$. The curve that fits the power spectrum for large frequencies is a function of the form

$$S(\omega) \sim \frac{1}{\omega^2}, \qquad \omega > \frac{1}{T}. \tag{3.102}$$

Note that in the figure we see a line and not a curve as the best fit since the scale is logarithmic. We shall not discuss this result in detail since it is not related to power-law statistics. We limit ourselves by saying that in the time region $t < T$, the waiting times τ have the same probability of occurring. The waiting time distribution in (3.31) is practically constant for $t \ll T$. Thanks to the coin-tossing prescription for the sign selection, the fluctuation $\xi(t)$ in this time region is virtually equivalent to the velocity fluctuations of the Langevin equation $dv/dt = -\gamma v(t) + f(t)$, with $f(t)$ denoting white noise and $\gamma \approx 1/T$, thereby yielding [33], $1/\omega^2$.

3.3.2 Interpretation of the Numerical Results

In order to reproduce the numerical results theoretically, we have to consider realisations with a finite length, L. Nevertheless, before we do so, we shall first develop a theoretical treatment for infinite realisations. In subsection 3.2.4 we calculated the

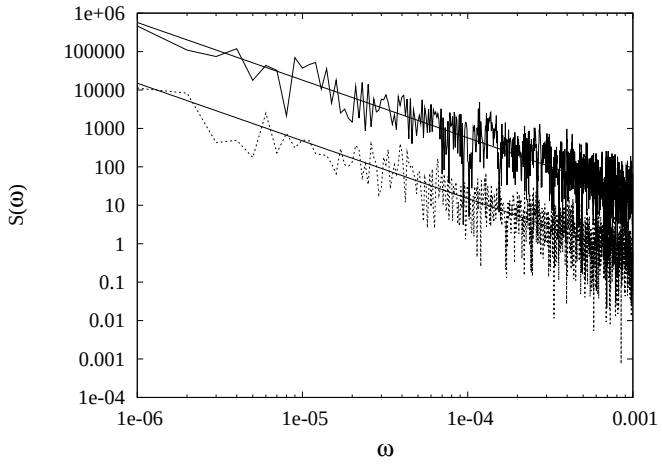

Figure 3.3: SINGLE REALIZATION. We used $\mu = 1.5 < 2$ for the two curves. The upper curve reppresents the power spectrum of a single realisation of length $L = 1 \times 10^7$ units. Increasing the length of the realisation to $L = 1 \times 10^9$ units makes the entire power spectrum drop to lower values. This is shown by the lower curve. The function that fits the upper curve is $0.00057\omega^{-1.5}$ and the one that fits the lower curve is $1.5 \times 10^{-5}\omega^{-1.5}$. This figure shows that the power spectrum of a single realisation is the same as the power spectrum of an ensemble of realisations.

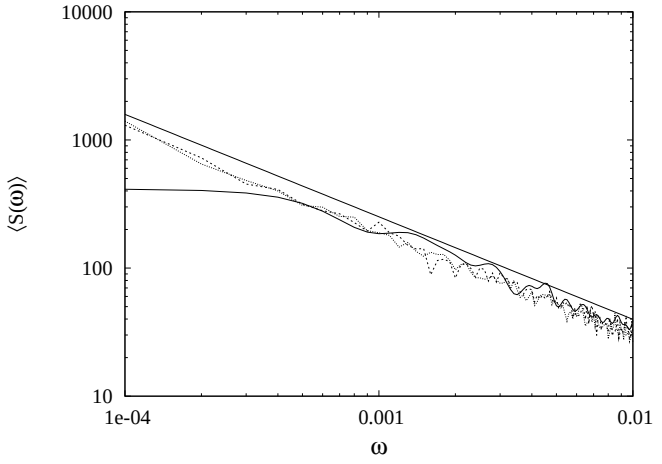

Figure 3.4: POWER-SPECTRUM - $\mu > 2$. We used $\mu = 2.2$ for all three curves in this figure. To each curve there corresponds a different realisation length L. Each curve was obtained by using an ensemble of 100 realisations. The full curve corresponds to an ensemble of realisations of length $L = 10^4$ units. The other two correspond to lengths $L = 10^5$ units and $L = 10^6$ units. The straight line is the function $\omega^{-0.8}$. The power-spectrum does not depend on the length, L, of the realisations.

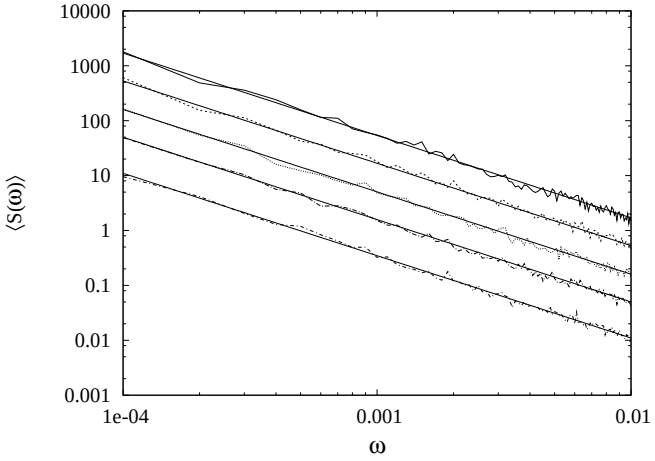

Figure 3.5: POWER-SPECTRUM - $\mu < 2$. We used $\mu = 1.5$ for all five curves in this figure - we are dealing with a non-stationary condition. To each curve there corresponds a different realisation length L. Each curve was obtained by using an ensemble of 1000 realisations. The topmost curve was realised using a realisation of length 10^6 units. The one immediately below corresponds to $L = 10^7$ units. As we move further below, the lengths of the realisations used were 10^8, 10^9 and 10^{10} units. The straight lines are functions of the form $K\omega^{-1.5}$, where K is a constant factor that dipends on the length, L of the sequence used (see Fig. 3.8). From top to bottom, $K = 1.7 \times 10^{-3}, \quad 5.3 \times 10^{-4}, \quad 1.6 \times 10^{-4}, \quad 5 \times 10^{-5}, \quad 1.1 \times 10^{-5}$.

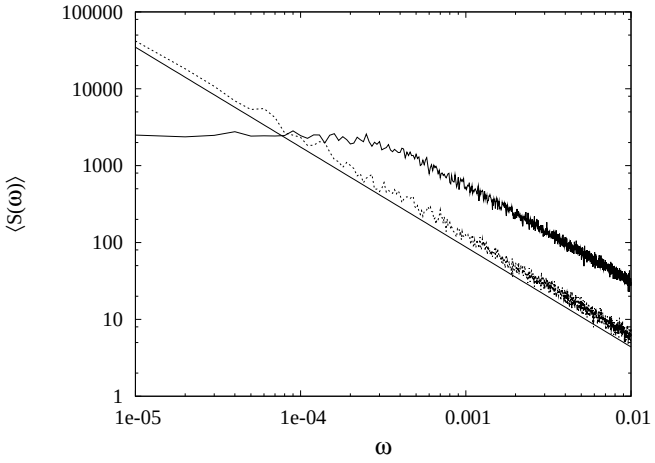

Figure 3.6: EFFECT OF TRUNCATING THE WAITING TIME DISTRIBUTION. We used $\mu = 1.7$ for this figure and an ensemble of 100 realisations for the curves. The waiting time distribution $\psi(\tau)$ was truncated at $\tau = 10^4$. In that case $T_{max} = 10^4$. The figure shows the power spectrum before and after truncation. The curve with the plateau corresponds to the truncated waiting time distribution. The straight line in the middle is $0.011\omega^{-1.3}$. Both curves were obtained using realizations of length $L = 10^6$.

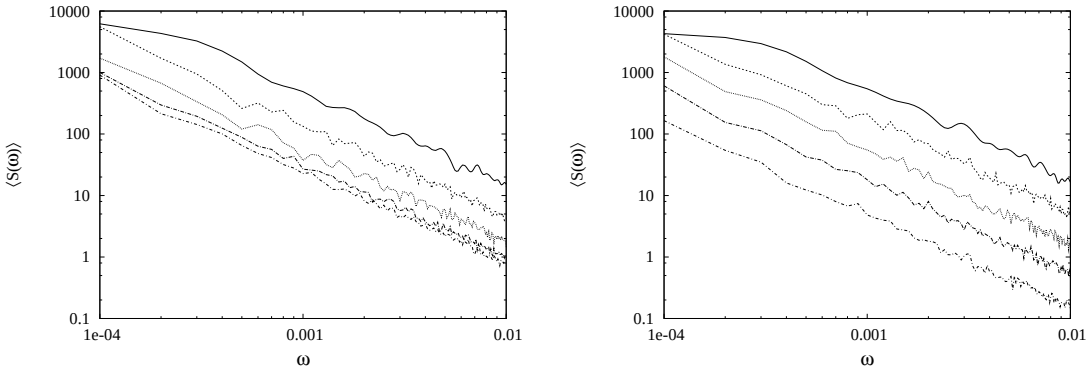

Figure 3.7: EFFECT OF TRUNCATING THE WAITING TIME DISTRIBUTION AND CHANGING L. Each curve in this figure is a result of averaging over 100 realizations. We used $\mu = 1.5 < 2$ for all the curves in these two figures. **Figure on the left:** we can see the effect of truncating the waiting time distribution $\psi(t)$. The topmost curve is the one created using the shortest realization length, L. As the length is increased, the curves drop. From top to bottom, the length of the realisations used is $L = 10^4$, 10^5, 10^6, 10^7, 10^8 units. We can see that they cease to do so after a certain limit (in fig. 3.8 this limiting value can be measured). Unlike in fig. 3.6, here we do not see a plateau because $\psi(\tau)$ was truncated at $\tau = 10^7 \gg 1/10^{-4}$. **Figure on the right:** it shows the result that is obtained under the same conditions as those used in the figure on the left, but without truncating the waiting time distribution.

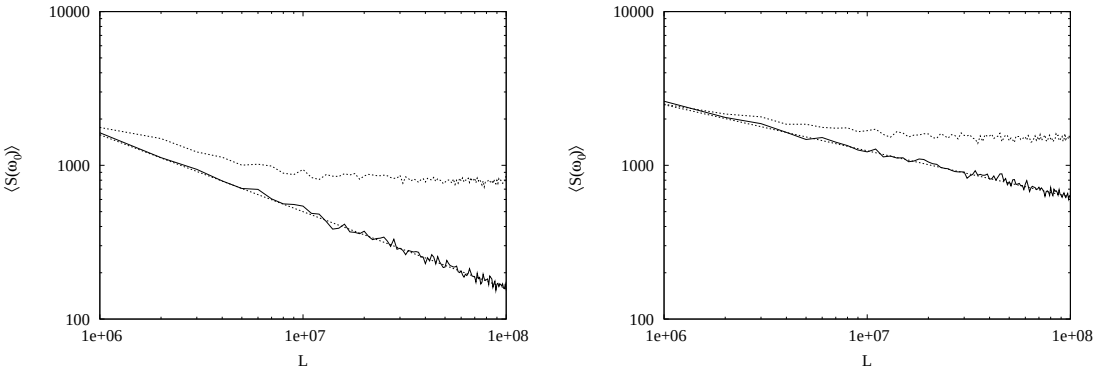

Figure 3.8: AMPLITUDE AS A FUNCTION OF REALIZATION LENGTH AT A CONSTANT FREQUENCY. **Both figures:** We used 1000 realisations. We fixed the angular frequency at $\omega_0 = 10^{-4}$ and calculated the corresponding amplitude $\langle S(\omega_0 = 10^{-4})\rangle$ for different realisation lengths L. The dashed curve is the result obtained when the waiting time distribution, $\psi(\tau)$ is truncated at $\tau = 10^7$. We see that after about $L = 10^7$ units, the power spectrum stops dropping as the realisation length increases. The full curve is the result obtained in the absence of truncation. **Figure on the left:** $\mu = 1.5$. The straight dashed line is a fit and corresponds to $1.58 \times 10^6 L^{-0.5}$. **Figure on the right:** $\mu = 1.7$. The straight dashed line is a fit and corresponds to $1.565 \times 10^5 L^{-0.3}$.

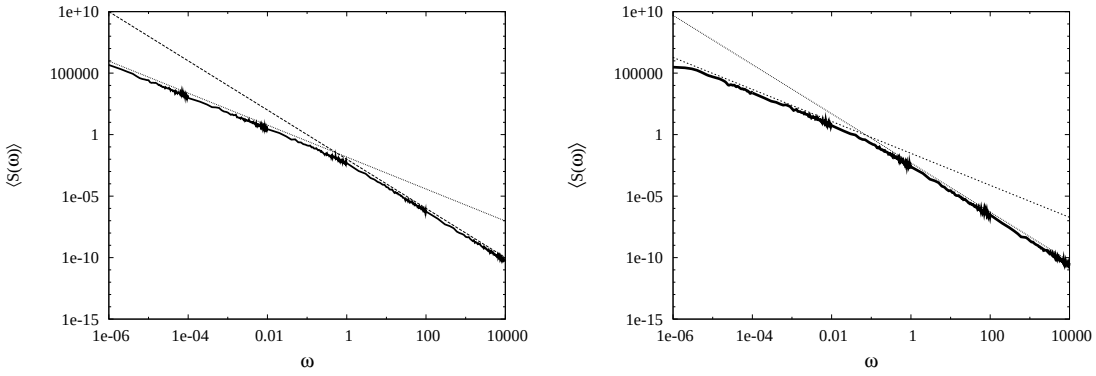

Figure 3.9: AVERAGE POWER SPECTRUM. We used $\mu = 1.7$ and 100 realizations of length $L = 10^7$ units. The figure shows the two regimes. **Figure on the left:** We used $T = 1$. The thick line is the numerical result. For $\omega < 1$, $\langle S(\omega)\rangle \propto 1/\omega^{3-\eta}$ and for $\omega > 1$, $\langle S(\omega)\rangle \propto 1/\omega^2$. The two finer lines that fit the numerical data are $0.015/\omega^{1.3}$ for $\omega < 1$ and $0.01/\omega^2$ for $\omega > 1$. The transition frequency is approximately equal to 1. **Figure on the right:** Same as the figure on the left the only difference being that $T = 10$. It shows that the transition frequency has moved to a lower value, approximately $\omega = 1/10 = 1/T$. The two finer lines that fit the numerical data are $0.03/\omega^{1.3}$ for $\omega < 1$ and $0.005/\omega^2$ for $\omega > 1$.

power spectrum of an infinitely long realisation, $\xi(t)$, with $\mu > 2$. For a stochastic process with $\mu < 2$, a different approach is necessary, one that is compatible with non-ergodicity. Using a Gibbs ensemble of realisations proves to be very effective. In subsection 3.2.3, with the help of a Gibbs ensemble, we showed that there exists a time-dependent correlation function even for non-ergodic systems. We are now going to develop this idea further.

Let us first study the case where $\mu > 2$. We consider an ensemble of realisations that are infinitely long. We prepare the ensemble so that each realisation starts with an event. We make sure that half of the them start with a positive laminar region and half with a negative laminar region, so that $\langle \xi(0)\rangle = 0$. In order to obtain the stationary condition we let the ensemble evolve for a very long time. After having done so, we select all the sequences characterised by $\xi(\infty) = 1$. In that way, we place the entire ensemble out of equilibrium from a stationary condition and we can calculate the autocorrelation function just like in subsection 3.2.3. The ensemble is expected to regress to the vanishing value from this macroscopic out-of-equilibrium situation as the corresponding correlation function of $\xi(t)$. From Eq. (3.61) we see that the correlation function is equal to the infinitely aged survival probability. The

Fourier transform of $\xi(t)$ is given by setting $N \to \infty$ in Eq. (3.97),

$$\hat{\xi}(\omega) = \frac{1}{\omega}\sin(\omega t_1) + \frac{i}{\omega}[1 - \cos(\omega t_1)] + R(t_2, t_3, \ldots). \tag{3.103}$$

Due to the random choice of the sign, we have that $\langle(\pm)_n\rangle = 0$ for every n that is different from zero. Consequently, $\langle R(t_2, t_3, \ldots)\rangle = 0$ and

$$\langle\hat{\xi}(\omega)\rangle = \frac{1}{\omega}\int_0^\infty \sin(\omega\tau)\psi_\infty(\tau)d\tau + \frac{i}{\omega}\int_0^\infty [1 - \cos(\omega\tau)]\psi_\infty(\tau)d\tau. \tag{3.104}$$

Taking the real part of $\langle\hat{\xi}(\omega)\rangle$ yields,

$$\Re\langle\hat{\xi}(\omega)\rangle = \frac{1}{\omega}\int_0^\infty \sin(\omega\tau)\psi_\infty(\tau)d\tau = -\frac{1}{\omega}\int_0^\infty \sin(\omega\tau)\frac{d}{dt}\Psi_\infty(\tau)d\tau, \tag{3.105}$$

where we have used the general property,

$$\Psi(\tau) = -\frac{d}{dt}\psi(\tau). \tag{3.106}$$

Integrating by parts gives

$$\begin{aligned}\Re\langle\hat{\xi}(\omega)\rangle &= \frac{1}{\omega}[-\sin(\omega\tau)\Psi_\infty(\tau)]_0^\infty + \int_0^\infty \cos(\omega\tau)\Psi_\infty(\tau)d\tau \\ &= \int_0^\infty \cos(\omega\tau)\Psi_\infty(\tau)d\tau.\end{aligned} \tag{3.107}$$

Using Eq. (3.83) and the Wiener-Khinchin theorem, we can conclude that

$$\langle S(\omega)\rangle = \Re\langle\hat{\xi}(\omega)\rangle = \int_0^\infty \cos(\omega\tau)\Psi_\infty(\tau)d\tau = \int_0^\infty \cos(\omega\tau)\Phi_\xi(\tau)d\tau. \tag{3.108}$$

We placed $S(\omega)$ under the Gibbs average operator, $\langle\ldots\rangle$ because the correlation function $\Phi_\xi(\tau)$ was obtained using an ensemble. On the other hand, in Eq. (3.83), the time average was used. Now, we want to extend this result to the general case that includes non-ergodic systems. We procede in the same way as above. We consider a Gibbs ensemble of prepared realisations, so that at $t = 0$, half of them are in the positive state ($|+\rangle$) and the other half in the negative state ($|-\rangle$). We let the ensemble evolve for a finite amount of time, upto $t = t_a < \infty$. At this time, we

select all the sequences characterised by $\xi(t_a) = 1$. For simplicity, we set t_a as the new origin of time. The sum of all these realisations corresponds to a macroscopic out-of-equilibrium fluctuation. In subsection 3.2.3 we saw that an ensemble created in such a way will decay to the vanishing value as the corresponding autocorrelation function of the fluctuation $\xi(t)$ (Eq. (3.60)). Even in this case, Eq. (3.103) is valid, and the Gibbs mean becomes

$$\langle\hat{\xi}(\omega)\rangle = \frac{1}{\omega}\int_0^\infty \sin(\omega\tau)\psi_{t_a}(\tau)d\tau + \frac{i}{\omega}\int_0^\infty [1-\cos(\omega\tau)]\psi_{t_a}(\tau)d\tau, \tag{3.109}$$

where $\psi_{t_a}(\tau)$ is the distribution density of the time distance between the time we start observing and the first event occurrence. We saw that in the stationary case, taking the real part of $\langle\hat{\xi}(\omega)\rangle$ conducted us to the Wiener-Khinchin theorem (Eq. (3.108)). In the general case, we have that

$$\langle S(\omega)\rangle = \Re\langle\hat{\xi}(\omega)\rangle = \frac{1}{\omega}\int_0^\infty \sin(\omega\tau)\psi_{t_a}(\tau)d\tau = \int_0^\infty \cos(\omega\tau)\Psi_{t_a}(\tau)d\tau. \tag{3.110}$$

This is a generalisation of the Wiener-Khinchin theorem in the case of infinitely long realisations, macroscopically perturbed at $t = t_a$. If we consider a process with $2 < \mu < \infty$, its power spectrum can be calculated using Eq. (3.110) when $t_a < \infty$. If we let $t_a \to \infty$, we recover the ordinary Wiener-Khinchin theorem, Eq. (3.108).

The fact is that the numerical results were obtained using finite sequences. Moreover, they show that for $\mu < 2$ the power spectrum depends on the length of the sequence used (Figs. 3.5 and 3.8). If we go back to subsection 3.2.4 we can see that the correlation function of an infinite sequence is equal to the infinitely aged survival probability function, $\Psi_\infty(\tau)$. Since we had only one sequence, we used the method of moving a window throughout the entire sequence. When the sequences are finite, we have to take into consideration the effects of rejuvenation, discussed in subsection 3.2.2. Let us therefore assume that in the case of limited sequences, the correlation function to be used in Eq. (3.110) is $\Psi_L(\tau)$. In other words, we assume that the age of the survival probability to be used is equal to the length of the sequence. Another assumption that we are going to make is that $\tau \ll L$. Since the sequence is limited, we cannot expect time intervals that are greater than L. Therefore we will definitely have $\tau < L$. The reason for considering $\tau \ll L$ is due to the rejuvenation effect. The longer time intervals encountered by the mobile window will contribute

to the younger waiting time distributions because of this effect. Furthermore, since

$$\psi(\tau) \sim \frac{1}{\tau^{\mu}} \tag{3.111}$$

and

$$\psi_L(\tau) \sim \frac{1}{\tau^{\mu-1}}, \tag{3.112}$$

the younger waiting time distributions decay much faster than the older waiting time distributions and are thus surpressed. In conclusion, only the smaller time intervals will contribute to the resultant autocorrelation function. The greatest contribution to the autocorrelation function is offered by the oldest survival probability function. In contrast, when the sequence is infinite and $\mu > 2$, then only the infinitely aged survival probability function contributes to the autocorrelation funcition. This is because all the laminar regions in the sequence are much smaller than the sequence itself, which is infinite.

By substituting $t_a = L$ in Eq. (3.40), we obtain

$$\psi_L(\tau) = (2-\mu)\frac{(\tau+T)^{1-\mu} - (\tau+T+L)^{1-\mu}}{(T+L)^{2-\mu} - T^{2-\mu}}. \tag{3.113}$$

For $\tau \ll L$ and $1 < \mu < 2$, the equation above reduces to

$$\psi_L(\tau) = (2-\mu)\frac{(\tau+T)^{1-\mu}}{(T+L)^{2-\mu} - T^{2-\mu}} \propto \frac{1}{L^{2-\mu}}\frac{1}{(\tau+T)^{\mu-1}}. \tag{3.114}$$

Notice the coefficient $1/L^{2-\mu}$, it is equal to the fit that we used in Fig. (3.8). The function in Eq. (3.114) is already normalised. The corresponding autocorrelation function is

$$\Phi_\xi(\tau) = \Psi_L(\tau) = \frac{(T+L)^{2-\mu} - (T+\tau)^{2-\mu}}{(T+L)^{2-\mu} - T^{2-\mu}}. \tag{3.115}$$

This correlation function is equal to the one obtained by Verberk et al. (Eq. (4), [46]). The approximation used causes the aged autocorrelation function in Eq. (3.114) to vanish at $\tau = L$. In the case of a set of Gibbs systems prepared at $t = 0$, with the out-of-equilibrium condition generated at $t = t_a$, the correlation function cannot vanish at $\tau = t_a$ and values of τ larger than t_a are permitted. This requires

the adoption of infinitely extended sequences. In the case of sequences of finite size L, vanishing of the correlation function at $\tau = L$ is a compelling consequence of L being finite.

For an analytical treatment of the power spectrum it is convenient to use the waiting time distribution $\psi_L(\tau)$, rather than the aging correlation function $\Psi_L(\tau)$. We note that $\psi_L(\tau)$ at $\tau = L$ undergoes an abrupt jump to 0, so as to fit Eq. (3.114). Thus, Eq. (3.110) has to be expressed as

$$\langle S(\omega)\rangle = \frac{1}{\omega}\int_0^L \sin(\omega\tau)\psi_L(\tau)d\tau. \tag{3.116}$$

By substituting (3.114) into the equation above yields

$$\langle S(\omega)\rangle = \frac{(2-\mu)}{\omega[(T+L)^{2-\mu} - T^{2-\mu}]}\int_0^L \sin(\omega\tau)(\tau+T)^{1-\mu}d\tau. \tag{3.117}$$

Since T is usually very small, much smaller than L, we have

$$\langle S(\omega)\rangle = \frac{(2-\mu)}{\omega L^{2-\mu}}\int_0^L \sin(\omega\tau)\tau^{1-\mu}d\tau. \tag{3.118}$$

Using the substitution $y = \omega\tau$, we have

$$\begin{aligned}\langle S(\omega)\rangle &= \frac{(2-\mu)}{\omega L^{2-\mu}}\int_0^{\omega L} \sin(y)\left(\frac{y}{\omega}\right)^{1-\mu}\frac{dy}{\omega} \\ &= \frac{(2-\mu)}{\omega^{3-\mu}L^{2-\mu}}\int_0^{\omega L}\sin(y)y^{1-\mu}dy \\ &\equiv A(\omega,L)(2-\mu)\frac{1}{L^{2-\mu}}\frac{1}{\omega^{3-\mu}} \\ &\propto \frac{1}{L^{2-\mu}}\frac{1}{f^{3-\mu}},\end{aligned} \tag{3.119}$$

where $A(\omega, L)$ is a slowly changing function of ω. This formula accounts very well for the numerical results in subsection 3.3.1. In fact, we can see that

$$\eta = 3 - \mu, \tag{3.120}$$

and that the power spectrum is proportional to $1/L^{2-\mu}$. These are two important results of the numerical simulations and the thesis itself. We can now also explain why the curves in Fig. (3.8) (the one on the left) accumulate. As we mentioned at

the beginning of this section, the effect of truncating a waiting time distribution is the creation of a well-defined first moment, even in the case where $\mu < 2$. When the length of the sequence becomes much greater than the mean time, aging stops due to the rejuvenation effect. The waiting time distribution, in a sense, becomes infinitely old prematurely and its age is no longer determined by the length of the sequence.

In order to calculate the power spectrum for $2 < \mu < 3$, we have to start from Eq. (3.113):

$$\psi_L(\tau) = (2-\mu)\left[\frac{1}{(\tau+T)^{\mu-1}} - \frac{1}{(\tau+T+L)^{\mu-1}}\right]\left[\frac{1}{(T+L)^{\mu-2}} - \frac{1}{T^{\mu-2}}\right]^{-1}. \quad (3.121)$$

If we assume that $\tau \ll L$, then

$$\psi_L = (\mu-2)\frac{T^{\mu-2}}{(\tau+T)^{\mu-1}} \equiv \psi_\infty(\tau). \quad (3.122)$$

In this case, there is no need to go further. The resulting power spectrum is identical to the one obtained using an infinite sequence, Eq. (3.89) or (3.92). The power spectrum does not depend on the length of the realisation when $\mu > 2$, in perfect agreement with the results shown in Fig. (3.4).

CHAPTER 4

Conclusion

We saw in the first part of the thesis that a Poisson system responds to a periodic forcing, giving rise to stochastic resonance. However, the adoption of the term *resonance* does not seem to be quite proper. This is because the resonance effect is obtained only if the rate of the system involved depends non-linearly on some other physical quantity, such as the temperature. This turned out to be a problem when we tried to extend the theory underlying stochastic resonance to the interaction of two Poisson systems. In general, such systems are characterised by the rates g_S and g_P, which themselves do not depend on other physical quantities. The only conclusion that we can make from our results is that the quality with which the perturbing signal is reproduced by the system depends on how much faster g_S is with respect to g_P. We discovered that this dependence is monotonous, the ideal case being when $g_S \to \infty$. Therefore, if we use the Gibbs ensemble perspective to study the interaction of Poisson systems, whose rates are not related to other properties, we will not see a resonance. Nevertheless, when we used single realisations, we were able to find the rate matching condition. We found that the condition $g_S = g_P$ is the boarder between the regime where the system events are attracted by the perturbation events, $g_S < g_P$, and the regime where the system events are repelled by the perturbation events $g_S > g_P$.

The main result of the second part is that the ideal $1/f$ condition is a singularity

corresponding to $\mu = 2$. This is the border between the ergodic ($\mu > 2$) and non-ergodic ($\mu < 2$) [35] condition. In other words, system with a power spectrum that is exactly of the form $1/f$, lie on the border between the ergodic and non-ergodic condition. The accurate evaluation of η, see Eq. (3.120), is expected to be a reliable criterion to establish which condition applies. It is worth noting that Eq. (3.40) applies to both cases, when μ is slightly larger as well as slightly smaller than 2.

Furthermore, we generalised the Wiener-Khinchin theorem by substituting the ordinary correlation function with a survival property of age L, where L is the length of the sequence studied. This has the effect of rendering the intensity of the power spectrum proportional to $1/L^{2-\mu}$. The same waiting time distribution of age L is used as the memory kernel in the generalised fluctuation-dissipation (FDT) theorem introduced by the authors of Ref. [47]. Essentially, the memory kernel in Eq. (2.28), relative to the Poisson case,

$$\chi(t,t') = g_S \exp\left[-g_s(t-t')\right] = \frac{d}{dt'} \exp\left[-g_s(t-t')\right] = \frac{d}{dt'}\Phi_\xi(t-t') \tag{4.1}$$

has to be replaced with

$$\chi(t,t') = \psi(t,t') = -\frac{d}{dt}\Psi(t,t') = -\frac{d}{dt}\Phi_\xi(t,t') \tag{4.2}$$

when we study the interaction between two complex systems ($1 < \mu < 2$). Hence, complexity matching and the power spectrum of non-ergodic systems are linked via the aged waiting time distribution. Eq. (4.1) expresses the standard FDT theorem whilst Eq. (4.2) expresses the generalised one. Note that in the non-equilibrium condition, Eq. (4.2), the derivative with respect to t is not equal to deriving with respect to t' and multiplying by -1. The form of $\chi(t,t')$ depends also on the absolute time distance from the time origin, where the preparation is done. The new FDT holds true even if the stationary condition is not realised. When $\mu < 2$, the process is always non-stationary and the generalisation of the Wiener-Khinchin theorem is done using the waiting time distribution density $\psi(t,t')$ that plays the role of a linear response function in the new FDT. If the system is prepared at $t = 0$, then $\psi(t,t')$ is the waiting time distribution of age t'.

In their article, Barbi et al. [1], extended stochastic resonance to the non-Poisson case and showed that the stochastic resonance dies out when the aging condition applies. In other words, they replaced the stationary waiting time distribution,

$g\exp(-g\tau)$, in Eq. (2.13) with an aged waiting time distribution characterised by $\mu < 2$. They used the same sinusoidal perturbation, $\cos(\omega t)$ with intensity ε. What they found was that the condition $\mu < 2$ annihilated the response coherence in the long time limit:

$$\Pi(t) \approx \varepsilon \frac{\cos\left(\frac{\pi}{2}\mu + \omega t\right)}{\Gamma(\mu-1)(\omega t)^{2-\mu}}. \tag{4.3}$$

This observation motivated us to reconsider the problem, but with a different perturbation. Instead of using a deterministic signal such as $\cos(\omega t)$, we considered using another complex system as the perturbation. The idea is that a complex system will respond only to another complex system, giving rise to complexity matching. In chapter 2 of the thesis we presented the results obtained from our study of the interaction of two Poisson systems. That was the first step towards a theory o complexity matching. At the moment progress is being made in the study of the interaction of complex systems.

The age dependent Wiener-Khinchin theorem of this article, see Eq. (3.116), yields a small dependence of the spectrum on L also in the case $\mu > 2$, in good agreement again with the numerical results. This is a consequence of the temporary aging of the condition $2 < \mu < 3$ [18] which fades away with increasing L until it recovers the ordinary ergodic prediction of L independence.

It is plausible that $T_{max} < \infty$ (truncated waiting time distribution) in all the physical processes generating intermittent fluorescence [48, 49], thereby generating the condition of interrupted aging [49] that ensures the validity of the traditional version of Wiener-Khinchin theorem. However, our results are expected to bring useful indications also in this case, insofar as the dependence of the spectral intensity on L that should be experimentally assessed for $L < T_{max}$, can be used to confirm the physical truncation of the waiting time distribution $\psi(\tau)$ at $\tau = T_{max}$. For this reason the theoretical work of presented in this thesis might help the progress of the experimental and theoretical research work in the field on intermittent fluorescence.

APPENDIX A

Wiener-Khinchin Theorem

We consider a stationary stochastic process whose corresponding time-series is given by the function $\xi(t)$. We assume that the time-series is finite of length L. In that case we have

$$\xi(t;L) = \begin{cases} \xi(t) & -L/2 \leq t \leq L/2 \\ 0 & \text{otherwise.} \end{cases} \tag{A.1}$$

whose Fourier-transform is given by

$$\hat{\xi}(\omega;L) = \mathcal{F}[\xi(t;L)] = \int_{-\infty}^{\infty} \xi(t;L)e^{i\omega t} = \int_{-L}^{L} \xi(t)e^{i\omega t}. \tag{A.2}$$

The power-spectrum of $\xi(t)$ is defined as

$$S(\omega) = \lim_{L\to\infty} \frac{1}{L}\hat{\xi}^*(\omega;L)\hat{\xi}(\omega;L) \tag{A.3}$$

Substituting (A.2) into (A.3) we have,

$$S(\omega) = \lim_{L\to\infty} \frac{1}{L}\int_{-\infty}^{\infty} dt_2 \int_{-\infty}^{\infty} dt_1 \xi(t_2;L)\xi(t_1;L)e^{i\omega(t_2-t_1)}. \tag{A.4}$$

Using the substitution $\tau = t_2 - t_1$ where t_1 is used as a parameter,

$$\begin{aligned} S(\omega) &= \int_{-\infty}^{\infty} d\tau e^{i\omega\tau} \lim_{L\to\infty} \frac{1}{L} \int_{-\infty}^{\infty} dt_1 \xi(t_1+\tau; L)\xi(t_1; L) \\ &= \int_{-\infty}^{\infty} d\tau e^{i\omega\tau} \overline{\xi(t_1+\tau)\xi(t_1)}, \end{aligned} \tag{A.5}$$

where the overline denotes the time average,

$$\overline{\xi(t_1+\tau)\xi(t_1)} \equiv \lim_{L\to\infty} \frac{1}{L} \int_{-\infty}^{\infty} dt_1 \xi(t_1+\tau; L)\xi(t_1; L). \tag{A.6}$$

If we assume that the process is stationary, the stochastic properties will not change as we shift along the time series. Therefore, we expect that the time average $\overline{\xi(t_1+\tau)\xi(t_1)}$ should be equal to the statistical average $\langle \xi(t_1+\tau)\xi(t_1)\rangle$ in which we average the product $\xi(t_1+\tau)\xi(t_1)$ at a given point $t = t_1$ over an infinite number of realisations of the time series $\xi(t)$. Hence, for a stationary process, we expect that the correlation function has the following property:

$$\Phi_\xi(\tau) \equiv \langle \xi(t_1+\tau)\xi(t_1)\rangle = \overline{\xi(t_1+\tau)\xi(t_1)}. \tag{A.7}$$

By substituting (A.7) into (A.5) we get

$$S(\omega) = \int_{-\infty}^{\infty} d\tau e^{i\omega\tau} \Phi_\xi(\tau). \tag{A.8}$$

In other words, we can say that for stationary processes, the power-spectrum is the Fourier-transform of the autocorrelation function. Eq.(A.7) is known as the *Wiener-Khinchin theorem*.

Bibliography

[1] F. Barbi, M. Bologna and P. Grigolini, Phys. Rev. Lett., **95**, 220601 (2005).

[2] W. A. C. Mutch, Fluctuations and Noise in Biological, Biophysical, and Biomedical Systems III, edited by N. G. Stocks, D. Abbott, R. P. Morse, Proc. of SPIE, Vol. 5841, 1 (2005).

[3] R. Soma, D. Nozaki, S. Kwak and Y. Yamamoto, Phys. Rev. Lett. **91**, 078101 (2003).

[4] Y. Yu, R. Romero and T. S. Lee, Phys. Rev. Lett. **94**, 108103 (2005).

[5] M. Buiatti, D. Papo, P.-M. Baudonniére and C. Van Vreeswijk, Neuroscience, **146**, 1400 (2007).

[6] A. K. Anderson, From Molecules to Mindfulness, Consciousness & Emotions, **1**, 193 (2000); R. Soma, D. Nozaki, S. Kwak, and Y. Yamamoto, Phys. Rev. Lett. **91**, 078101 (2003).

[7] D. Deligniéres, K. Torre, L. Lemaine, Acta Psychologica **127**, 328 (2008); D. Deligniéres, L. Lemaine, K. Torre, Human Movement Science **23**, 87 (2004); H. Kadota, K. Kudo, T. Ohtsuki, Neuroscience Letters **370**, 97 (2004); A. Paraschiv-Ionescu, E. Buchser, B. Rutschmann and K. Aminian, Phys. Rev. E **77**, 021913 (2008).

[8] W. Paul and J. Baschnagel, Shochastic Processes: From Physics to Finance, Springer (1999).

[9] M. Luković, M. Ignaccolo, L. Fronzoni, P. Grigolini, Phys. Lett. A, **372**, 2608 (2008).

[10] H. A. Kramers, Physica VII, no. 4, 284 (1940).

[11] B. McNamara and K. Wiesenfeld, Phys. Rev. A, **39**, 4854 (1989).

[12] L. Gammaitoni, P. Hänggi and P. Jung, Rev. Mod. Phys., **70**, 223 (1998).

[13] B. Percha, R. Dzakpasu, and M. Zocchowski, Phys. Rev. E **72**, 031909 (2005); M. Zochowski and R. Dzakpasu, J. Phys. A **37**, 3823 (2004).

[14] G. Zumofen and J. Klafter, Physica D, **69**, 436 (1993).

[15] T. Geisel, J. Nirwetberg and A. Zacherl, Phys. Rev. Lett., **54**, 616 (1985).

[16] P. Allegrini, G. Aquino, P. Grigolini, L. Palatella, A. Rosa, Phys. Rev. E, **68**, 056123 (2003).

[17] P. Allegrini, G. Aquino, P. Grigolini, L. Palatella, A. Rosa, B. West, Phys. Rev. E, **71**, 066109 (2005).

[18] G. Aquino, M. Bologna, P. Grigolini, and B. West, Phys. Rev. E, **70**, 036105 (2004).

[19] B. J. West, M. Bologna, and P. Grigolini, Physics of Fractal Operators Springer (2003).

[20] S. Bianco, P. Grigolini and P. Paradisi, J. Chem. Phys. **123**, 174704 (2005).

[21] L. Laloux and P. Le Doussal, Phys. Rev. E **57**, 6296, (1998); E. Barkai, Phys. Rev. Lett., **90**, 104101 (2003).

[22] C. W. Gardiner, Handbook of Stochastic Methods for Physics, Chemistry and the Natural Sciences, Second Enlarged Edition, Springer Series in Synergetics **13** , Springer (1990).

[23] M. Pelton, D. G. Grier, and P. Guyot-Sionnest, Applied Physics Letters, **85**, 819 (2004).

[24] M. Nirmal, B.O. Dabbousi, M.G. Bawendi, J.J. Macklin, J. K. Trautman, T. D. Harris, L. E. Brus, Nature **383**, 802 (1996).

[25] M. Kuno, D. P. Fromm, H. F. Hamann, A. Gallager, D. J. Nesbitt, J. Chem. Phys. **112**, 3117 (2000).

[26] K. T. Shimizu, R. G. Neuhauser, C. A. Leatherdale, S. A. Empedocles, W. K. Woo, M. G. Bawendi, Phys. Rev. B **63**, 205316 (2001).

[27] M. Haase, C. G. Hübner, E. Reuther, A. Herrmann, K. Müllen, T. Basche, J. Phys. Chem. B **108**, 10445 (2004).

[28] J. Schuster, F. Cichos, C. von Borczyskowski, Appl. Phys. Lett. **87**, 051915 (2005).

[29] J. P. Hoogenboom, E. M. H. P. van Dijk, J. Hernando, N. F. van Hulst, M. F. Garcia-Parajo, Phys. Rev. Lett. **95**, 097401 (2005).

[30] E. K. L. Yeow, S. M. Melnikov, T. D. M. Bell, F. C. De Schryver, J. Hofkens, J. Phys. Chem. A **110**, 1726 (2006).

[31] X. Brokmann, J. P. Hermier, G. Messin, P. Desbiolles, J. P. Bouchaud, M. Dahan, Phys. Rev. Lett. **90**, 120601 (2003).

[32] S. Bianco, P. Grigolini, and P. Paradisi J. Chem. Phys. **123**, 174704 (2005).

[33] R. F. Voss and J. Clarke, J. Acoust. Soc. Am. **63**, 258 (1978); Phys. Rev. **13**, 556 (1992).

[34] E. Barkai, Phys. Rev. Lett. **90**, 104101 (2003).

[35] G. Margolin, E. Barkai, Phys. Rev. Lett. **94**, 080601 (2005); E. Barkai, J. Stat. Phys. **123** 883 (2006); G. Bel, E. Barkai, Europhys Lett. **74**, 15 (2006); G. Bel, E. Barkai, J. Phys. Cond. Matt. **17**, S4287 (2005).

[36] G. Margolin, E. Barkai, J. Stat. Phys. **122**, 137 (2006)

[37] J. P. Hoogenboom, J. Hernando, E. M. H. P. van Dijk, N. F. van Hulst and M. F. García-Parajó, ChemPhysChem **8**, 823 (2007).

[38] M. Pelton, G. Smith, N. F. Scherer, and R. A. Marcus, Proc Natl Acad Sci USA, **104**, 14249 (2007).

[39] J. B. Johnson, Phys. Rev. **26**, 71 (1925).

[40] R. Möller, A. Esslinger, and B. Koslowski, J. Vac. Sci. Technol. A **8**, 590 (1990).

[41] L. E. Reichl, A Modern Course in Statistical Physics, Second Edition, John Wiley and Sons (1998).

[42] U. Weiss, Quantum Dissipative Systems, Series in Modern Condensed Matter Physics, World Scientific, second edition, 1999.

[43] I. S. Gradshteyn and I. M. Ryzhik, Table of Integrals, Series and Products, Academic Press, Corrected and Enlarged Edition, 1979.

[44] G. Zumofen and J. Klafter, Phys. Rev. E **47**, 851 (1993).

[45] A. Neiman, L. Schimansky-Geier and F. Moss, Phys. Rev. E **56**, R9 (1997).

[46] R. Verberk, A. M. van Oijen, and M. Orrit, Phys. Rev. B **66**, 233202 (2002).

[47] P. Allegrini, M. Bologna, P. Grigolini and B. J. West, Phys. Rev. Lett. **99**, 010603 (2007).

[48] I. Chung, J. M. Witkoskie, J. Cao, and M. G. Bawendi, Phys. Rev. E **73**, 011106 (2006).

[49] J. B. Witkoskie and J. Cao, J. Chem. Phys. **125**, 244511 (2006).